DE LA RECHERCHE À L'INDUSTRIE

Entropy stable and positivity-preserving Godunov-type schemes for multidimensional hyperbolic systems on unstructured grid

15th March 2022

PhD student: **Agnes Chan**[1,3], Supervisors: Raphaël Loubère[2], Pierre-Henri Maire[3]

Commissariat à l'énergie atomique et aux énergies alternatives - www.cea.fr

1. Université de Bordeaux, Institut de Mathématiques de Bordeaux(IMB), UMR5251, bordeaux INP - agnes.chan@u-bordeaux.fr
2. Université de Bordeaux, Institut de Mathématiques de Bordeaux(IMB), UMR5251, bordeaux INP
3. CEA Cesta, Le Barp

Goal

Numerical methods to simulate compressible flow.

Problem

Supersonic/hypersonic flow:
Flow with strong shock and rarefaction waves.

Methodology

1. **Model :**

Non-linear hyperbolic conservation laws :

Euler equations $\frac{\partial \mathbf{U}}{\partial t} + \nabla \cdot \mathbb{F}(\mathbf{U}) = \mathbf{0}$.

(Building block for Navier-Stokes equations.)

2. **Discretisation :**

Finite Volume method(FV) :

Godunov-type scheme

$$\frac{\mathbf{u}_i^{n+1} - \mathbf{u}_i^n}{\Delta t} + \frac{\mathbf{f}_{i+1/2}^n - \mathbf{f}_{i-1/2}^n}{\Delta x} = 0,$$

- $\mathbf{u}_i^n$: approximation of the solution $\mathbf{u}(t, x)$.
- $\mathbf{f}_{i+1/2} = \mathbf{f}(\mathbf{u}_i, \mathbf{u}_{i+1})$: numerical flux.

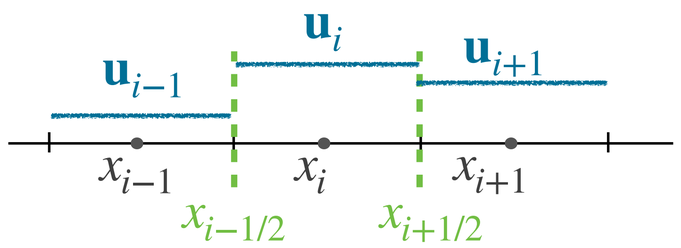

3. **Riemann solver :**

- Robust & accurate

3D simulation of Cone-cylinder-flare[0]

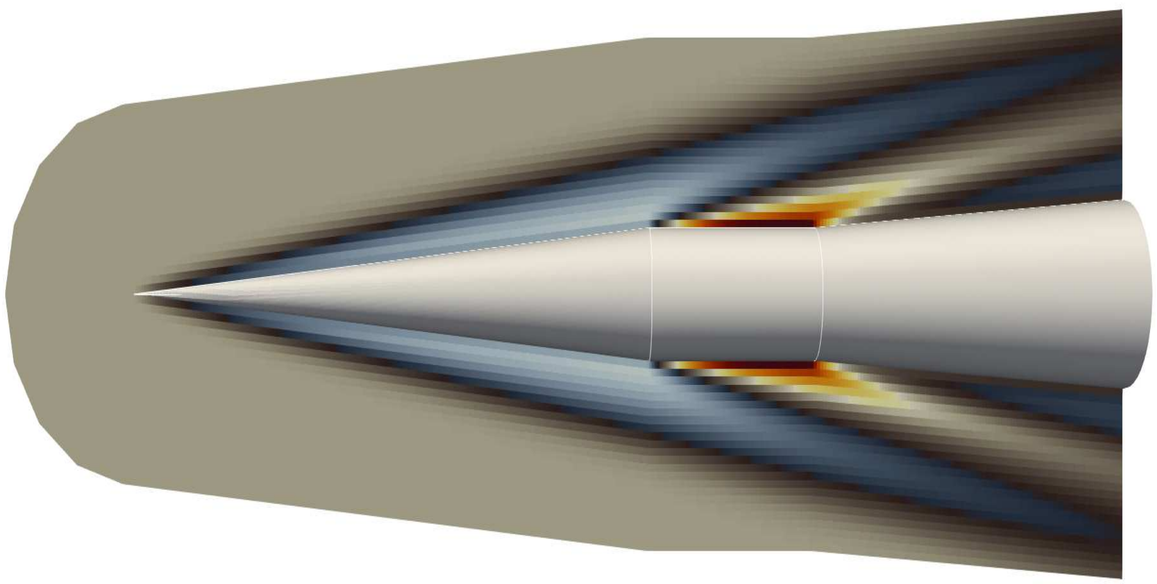

0. S. Esquieu, E. Benitez, S.P. Schneider, J-P. Brazie, Flow and Stability Analysis of a Hypersonic Boundary Layer over an Axisymmetric Cone-cylinder-flare Configuration, AIAA, 2019.

Riemann solvers (RS) - Brief history

Riemann problem introduced by Bernhard Riemann.	S.K. Godunov[1] used the exact solution of the Riemann problem as building block for FV scheme for compressible flow.	Development of approximate RS. i.e. Roe[2], HLL[3], HLLE, HLLC[4], Osher etc.	Attempt to develop multi-dimensional RS.	Improving properties of RS. i.e. Positivity-preserving, entropy stable.
1860	1959	1980 onwards	2000's	

Common feature: Eulerian framework

Different perspective:

- Resolution from the Lagrangian standpoint.

  (Re-interpretation of the work of Gallice[5].)

1. S. K. Godunov, « A Difference Scheme for Numerical Solution of Discontinuous Solution of Hydrodynamic Equations », Math. Sbornik, vol. 47, 1959, p. 271-306, translated US Joint Publ. Res. Service, JPRS 7226, 1969
2. P.L. Roe. Approximate Riemann solvers, parameter vectors, and difference schemes. J. Comput. Phys., 43:357–372, 1981.
3. A.Harten, P.D.Lax, and B.van Leer .On upstream Differencing and GodunovType schemes for Hyperbolic Conservation Laws. SIAM Review, 25(1):35–61, 1983.
4. E.F.Toro. Riemann Solvers and Numerical Methods for Fluid Dynamics. Springer, second edition,1999.
5. G. Gallice, Positive and entropy stable Godunov-type schemes for gas dynamics and MHD equations in Lagrangian or Eulerian coordinates, Numer. Math., 94(4):673-713, 2003.

Approach :

Re-interpretation of the work of Gallice[5] by:

Develop **Lagrangian RS** :
- Contact discontinuity preserving;
- Positivity-preserving;
- Entropy stable.

Lagrange-to-Euler mapping →

Develop **Eulerian counter-part** :
- Inherits the properties of Lagrangian RS;
- Explicit expression and direct estimation of waves speeds;
- Ordered wave speeds.

Outline :

1. 1D FV scheme :
   - Lagrangian scheme;
   - Eulerian scheme.
2. 2D FV scheme :
   - Generic multi-dimensional FV scheme;
   - Conservativity and node-based condition;
   - Test case validation.
3. Extensions of FV scheme.
4. Conclusion & Perspectives.

5. G. Gallice, Positive and entropy stable Godunov-type schemes for gas dynamics and MHD equations in Lagrangian or Eulerian coordinates, Numer. Math., 94(4):673-713, 2003.

1D Governing Equations[5,6]

1D Lagrangian gas dynamics

$$\frac{\partial \mathbf{V}}{\partial t} + \frac{\partial \mathbf{G}(\mathbf{V})}{\partial m} = \mathbf{0}$$

$$\mathbf{V} = (\tau, u, e)^t, \ \mathbf{G} = (-u, p, pu)^t$$

Eigenvalues : $-\frac{a}{\tau}, 0, \frac{a}{\tau},$

Entropy inequality : $-\frac{\partial \eta}{\partial t} \geq 0.$

1D Eulerian gas dynamics

$$\frac{\partial \mathbf{U}}{\partial t} + \frac{\partial \mathbf{F}(\mathbf{V})}{\partial x} = \mathbf{0}$$

$$\mathbf{U} = (\rho, \rho u, \rho e)^t, \quad \mathbf{F} = (\rho u, \rho u^2 + p, \rho u e + p u)^t$$

Eigenvalues : $u - a, u, u + a$

Entropy inequality : $\frac{\partial \rho\eta}{\partial t} + \frac{\partial}{\partial x}(\rho \eta u) \geq 0.$

Thermodynamic closure : $p(\tau, \eta) = -\frac{\partial \varepsilon}{\partial \tau}, \ \theta(\tau, \eta) = \frac{\partial \varepsilon}{\partial \eta},$

Fundamental Gibbs relation : $\theta d\eta = p d\tau + d\varepsilon,$

Isentropic sound speed : $\frac{a^2}{\tau^2} = -\frac{\partial p}{\partial \tau} = \frac{\partial^2 \varepsilon}{\partial \tau^2}$

Lagrange to Euler formulae

$$\mathbf{V} = \tau(\mathbf{U} - \rho \mathbf{e}_1) + \tau \mathbf{e}_1,$$

$$\mathbf{G} = \mathbf{F} - u\mathbf{U} - u\mathbf{e}_1,$$

With $\mathbf{e}_1 = (1,0,0)^t$.

5. G. Gallice, Positive and entropy stable Godunov-type schemes for gas dynamics and MHD equations in Lagrangian or Eulerian coordinates, Numer. Math., 94(4):673-713, 2003.

6..A . Chan, G. Gallice, R. Loubère, P.-H. Maire, Positivity preserving and entropy consistent approximate Riemann solvers dedicated to the high-order MOOD based finite-volume discretization of Lagrangian and Eulerian gas dynamics, Submitted 2021 to Computers & Fluids.

1D Lagrangian Riemann problem

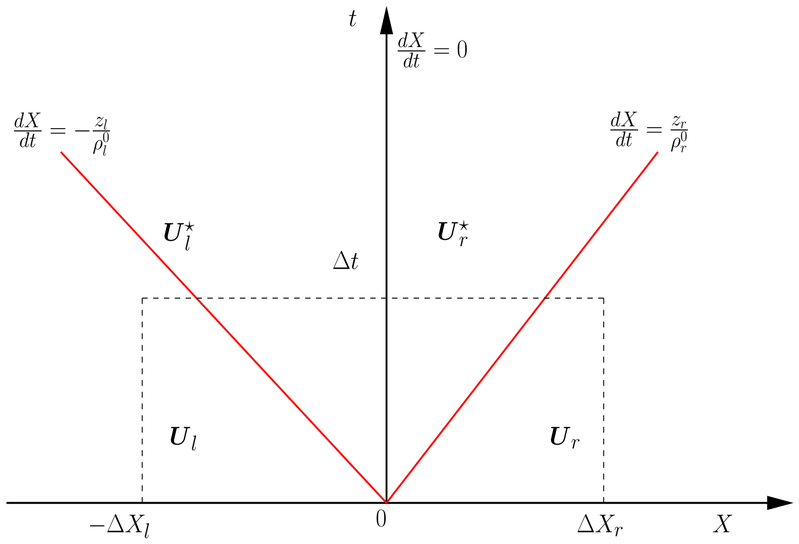

$$\frac{\partial \mathbf{V}}{\partial t}+\frac{\partial \mathbf{G}}{\partial m}=\mathbf{0},\quad \mathbf{V}(x,0)=\begin{array}{ll}\mathbf{V}_l \text{ if} & m<0,\\ \mathbf{V}_r \text{ if} & m\geq 0,\end{array}$$

Simple Lagrangian solver

Composed of 4 states : $\mathbf{V}_l, \mathbf{V}_r, \mathbf{V}_l^\star, \mathbf{V}_r^\star$,
Separated by 3 discontinuities : $-\lambda_l$, 0, λ_r.

$$\mathbf{W}(\mathbf{V}_l,\mathbf{V}_r,\frac{m}{t})=\begin{cases}\mathbf{V}_l \text{ if } \frac{m}{t}\leq -\lambda_l,\\ \mathbf{V}_l^\star \text{ if } -\lambda_l<\frac{m}{t}\leq 0,\\ \mathbf{V}_r^\star \text{ if } 0<\frac{m}{t}\leq \lambda_r,\\ \mathbf{V}_r \text{ if } \lambda_r<\frac{m}{t}.\end{cases}$$

1D Eulerian Riemann problem

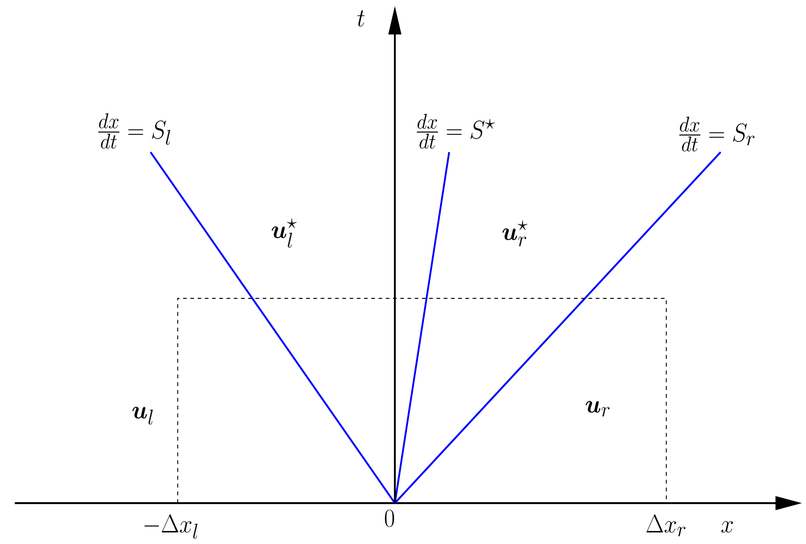

$$\frac{\partial \mathbf{U}}{\partial t}+\frac{\partial \mathbf{F}}{\partial x}=\mathbf{0},\quad \mathbf{U}(x,0)=\begin{array}{ll}\mathbf{U}_l \text{ if} & x<0,\\ \mathbf{U}_r \text{ if} & x\geq 0,\end{array}$$

Simple Eulerian solver

Construct from the simple Lagrangian solver with the **Lagrange-to-Euler mapping.**

5. G. Gallice, Positive and entropy stable Godunov-type schemes for gas dynamics and MHD equations in Lagrangian or Eulerian coordinates, Numer. Math., 94(4):673-713, 2003.
6..A . Chan, G. Gallice, R. Loubère, P.-H. Maire, Positivity preserving and entropy consistent approximate Riemann solvers dedicated to the high-order MOOD based finite-volume discretization of Lagrangian and Eulerian gas dynamics, Submitted 2021 to Computers & Fluids.

Lagrangian jump relations :

$$(\mathcal{S}_l)\begin{cases} \lambda_l(\tau_l^\star - \tau_l) - (u^\star - u_l) = 0, \\ \lambda_l(u^\star - u_l) + p_l^\star - p_l = 0, \\ \lambda_l(e_l^\star - e_l) + (p_l^\star u^\star - p_l u_l) = 0, \end{cases} \qquad (\mathcal{S}_r)\begin{cases} \lambda_r(\tau_r^\star - \tau_r) + (u^\star - u_r) = 0, \\ \lambda_r(u^\star - u_r) - (p_r^\star - p_r) = 0, \\ \lambda_r(e_r^\star - e_r) - (p_r^\star u^\star - p_r u_r) = 0, \end{cases}$$

Positivity and entropy control : Explicit condition on λ_l & λ_r

1. Positivity of intermediate specific volume $\tau_l^\star > 0$ and $\tau_r^\star > 0$:

$$\lambda_l = \max\left(\frac{a_l}{\tau_l}, \sqrt{\frac{[p]}{\tau_l}}, -\frac{[u]}{\tau_l}\right), \quad \lambda_r = \max\left(\frac{a_r}{\tau_r}, \sqrt{\frac{[-p]}{\tau_r}}, -\frac{[u]}{\tau_r}\right)$$

2. Positivity of intermediate internal energy $\varepsilon_l^\star > 0$ and $\varepsilon_r^\star > 0$:

For a convex EOS : $\quad \lambda_l \geq \frac{a_l}{\tau_l}, \;\; \lambda_r \geq \frac{a_r}{\tau_r}$

3. Entropy control $\eta_l^\star \geq \eta_l$ and $\eta_r^\star \geq \eta_r$:

$$\lambda_s \geq \frac{a(\tau, \eta_s)}{\tau}, \text{ for } \tau \in (\tau_s, \tau_s^\star) \text{ and } s = l, r$$

5. G. Gallice, Positive and entropy stable Godunov-type schemes for gas dynamics and MHD equations in Lagrangian or Eulerian coordinates, Numer. Math., 94(4):673-713, 2003.

6..A . Chan, G. Gallice, R. Loubère, P.-H. Maire, Positivity preserving and entropy consistent approximate Riemann solvers dedicated to the high-order MOOD based finite-volume discretization of Lagrangian and Eulerian gas dynamics, Submitted 2021 to Computers & Fluids.

Associated Lagrangian FV scheme :

$$\mathbf{V}_i^{n+1} = \mathbf{V}_i^n - \frac{\Delta t}{m_i}\left(\mathbf{G}^\star_{i+1/2} - \mathbf{G}^\star_{i-1/2}\right), \quad \mathbf{G}^\star_{i+1/2} = \begin{pmatrix} -u^\star_{i+1/2} \\ p^\star_{i+1/2} \\ p^\star_{i+1/2}u^\star_{i+1/2} \end{pmatrix}$$

With $$u^\star = \frac{\lambda_l u_l + \lambda_r u_r}{\lambda_l + \lambda_r} - \frac{[p]}{\lambda_l + \lambda_r}, \quad p^\star = \frac{\lambda_l p_r + \lambda_r p_l}{\lambda_l + \lambda_r} - \frac{\lambda_l \lambda_r}{\lambda_l + \lambda_r}(u_r - u_l)$$

Time step monitoring $$\Delta t = CFL \min_i \left(\frac{m_i}{\lambda_{r,i-1/2} + \lambda_{l,i+1/2}} \right)$$

Properties of Lagrangian FV scheme :

- First order in time and space;
- Positivity preserving;
- Entropy stability;

→ Building block for **Eulerian FV scheme!**

5. G. Gallice, Positive and entropy stable Godunov-type schemes for gas dynamics and MHD equations in Lagrangian or Eulerian coordinates, Numer. Math., 94(4):673-713, 2003.
6..A . Chan, G. Gallice, R. Loubère, P.-H. Maire, Positivity preserving and entropy consistent approximate Riemann solvers dedicated to the high-order MOOD based finite-volume discretization of Lagrangian and Eulerian gas dynamics, Submitted 2021 to Computers & Fluids.

Methodology and assumptions :

The simple Eulerian solver is constructed using the Lagrangian solver (**W**) with the **Lagrange-to-Euler mapping** and assuming that :

(H1) $\lambda_k(\tau_{k+1} - \tau_k) + u_{k+1} - u_k = 0$, for $k = 1 \ldots m$,

(H2) $\tau_k > 0$, for $k = 1 \ldots m$.

(H1) is nothing but the weak form of the mass/volume equation $\dfrac{\partial \tau}{\partial t} - \dfrac{\partial u}{\partial x} = 0$.

Construction of Eulerian wave speeds from the Lagrangian ones :

$\Lambda_k = u_k + \lambda_k \tau_k$, thanks to (H1), and by virtue of (H1) the Eulerian wave speeds are ordered.

5. G. Gallice, Positive and entropy stable Godunov-type schemes for gas dynamics and MHD equations in Lagrangian or Eulerian coordinates, Numer. Math., 94(4):673-713, 2003.

6..A . Chan, G. Gallice, R. Loubère, P.-H. Maire, Positivity preserving and entropy consistent approximate Riemann solvers dedicated to the high-order MOOD based finite-volume discretization of Lagrangian and Eulerian gas dynamics, Submitted 2021 to Computers & Fluids.

Summary of the Eulerian RS:

Composed of 4 states : $\mathbf{U}_l, \mathbf{U}_r, \mathbf{U}_l^\star, \mathbf{U}_r^\star$,
Separated by 3 discontinuities : $-\Lambda_l$, Λ_0, Λ_r.

$$\mathbf{W}^{eul}(\mathbf{U}_l, \mathbf{U}_r, \frac{x}{t}) = \begin{cases} \mathbf{U}_l & \text{if} \quad \frac{x}{t} < \Lambda_l, \\ \mathbf{U}_l^\star & \text{if} \quad \Lambda_l, < \frac{x}{t} < \Lambda_0, \\ \mathbf{U}_r^\star & \text{if} \quad < \Lambda_0, \frac{x}{t} < \Lambda_r, \\ \mathbf{U}_r & \text{if} \quad \Lambda_r < \frac{x}{t}. \end{cases}$$

$$\mathbf{U}_s \begin{pmatrix} \rho_s \\ \rho_s u_s \\ \rho_s e_s \end{pmatrix} \qquad \mathbf{U}_s^\star = \begin{pmatrix} \rho_s^\star \\ \rho_s^\star u_s^\star \\ \rho_s^\star e_s^\star \end{pmatrix}$$

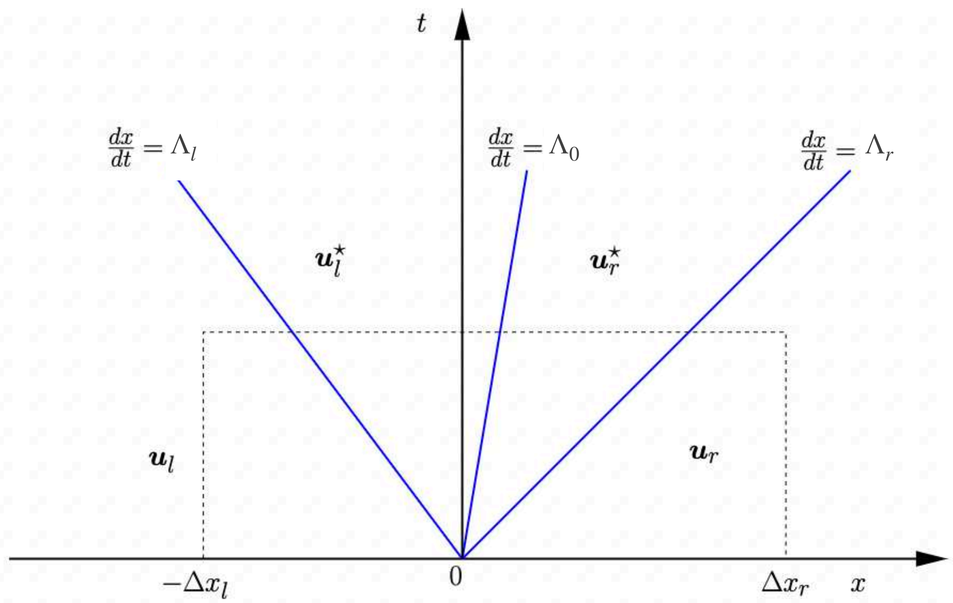

1. Compute Lagrangian wave speeds : λ_l and λ_r

   - Inherit the properties from the Lagrangian solver.

2. Compute Eulerian wave speeds Λ_l and Λ_0 and Λ_r:

   - $\Lambda_l = -\lambda_l \tau_l + u_l = -\lambda_l \tau_l^\star + u^\star$;
   - $\Lambda_o = u^\star$,
   - $\Lambda_r = \lambda_r \tau_r + u_r = -\lambda_r \tau_r^\star + u^\star$

3. Compute intermediate states : $\rho_s^\star, p_s^\star, e_s^\star, s = l, r$

   - Using Lagrangian RS.

$$p_l^\star = p_l + \lambda_l (u_l - u^\star)$$

$$\rho_l^\star = \frac{\lambda_l \rho_l}{\rho_l (u^\star - u_l)} + \lambda_l \qquad e_l^\star = e_l + \frac{p_l u_l - p^\star u^\star}{\lambda_l}$$

$$\rho_r^\star = \frac{\lambda_r \rho_r}{\rho_r (u_r - u^\star)} + \lambda_r \qquad e_r^\star = e_r - \frac{p_r u_r - p^\star u^\star}{\lambda_r}$$

5. G. Gallice, Positive and entropy stable Godunov-type schemes for gas dynamics and MHD equations in Lagrangian or Eulerian coordinates, Numer. Math., 94(4):673-713, 2003.
6..A . Chan, G. Gallice, R. Loubère, P.-H. Maire, Positivity preserving and entropy consistent approximate Riemann solvers dedicated to the high-order MOOD based finite-volume discretization of Lagrangian and Eulerian gas dynamics, Submitted 2021 to Computers & Fluids.

Associated Eulerian FV scheme :

$$\mathbf{U}_i^{n+1} = \mathbf{U}_i^n - \frac{\Delta t}{x_i}\left(\mathbf{F}^\star_{i+1/2} - \mathbf{F}^\star_{i-1/2}\right),$$

Numerical flux :$\mathbf{F}^\star = \frac{1}{2}(\mathbf{F}_l + \mathbf{F}_r) - \frac{\Lambda_l}{2}(\mathbf{U}_l^\star - \mathbf{U}_l) - \frac{\Lambda_0}{2}(\mathbf{U}_r^\star - \mathbf{U}_l^\star) - \frac{\Lambda_r}{2}(\mathbf{U}_r - \mathbf{U}_r^\star).$

Time step monitoring $\Delta t = CFL \dfrac{\Delta x_i}{\max_i \left(|u_i^n| + \dfrac{\lambda_{r,i-1/2} + \lambda_{l,i+1/2}}{\rho_i^n} \right)}$

Properties of Eulerian FV scheme :

- First order in time and space;
- Positivity preserving;
- Entropy stability;
- Explicit expression for Eulerian wave speeds;
- Wave speeds ordering.

5. G. Gallice, Positive and entropy stable Godunov-type schemes for gas dynamics and MHD equations in Lagrangian or Eulerian coordinates, Numer. Math., 94(4):673-713, 2003.

6..A . Chan, G. Gallice, R. Loubère, P.-H. Maire, Positivity preserving and entropy consistent approximate Riemann solvers dedicated to the high-order MOOD based finite-volume discretization of Lagrangian and Eulerian gas dynamics, Submitted 2021 to Computers & Fluids.

Method :

Space discretisation:

Polynomial reconstruction from 1st to 5th degree + MOOD limiting.

Time discretisation:

Runge-Kutta method

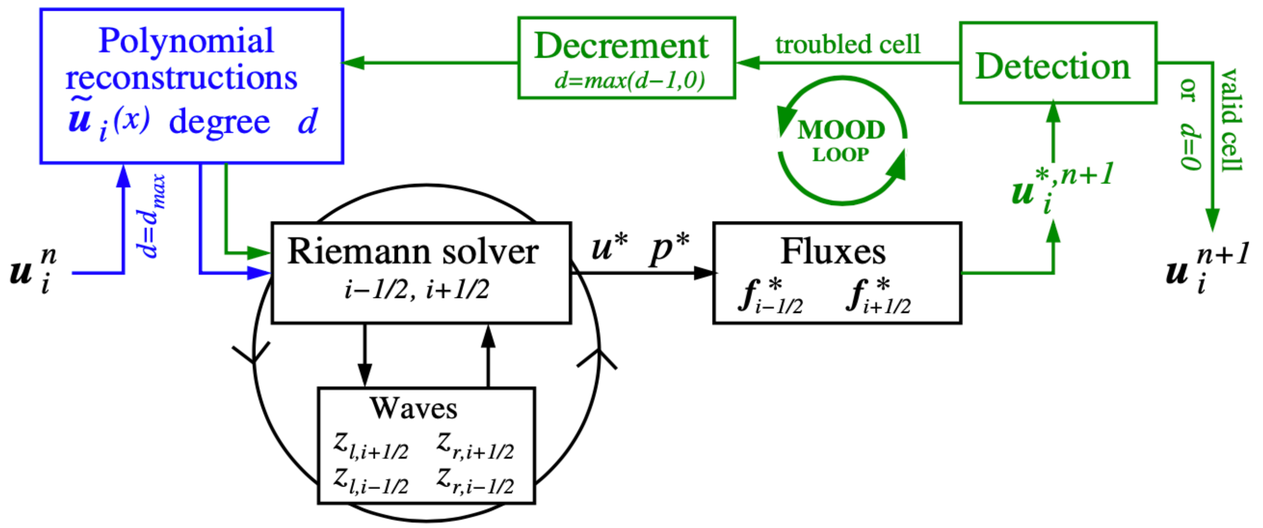

High-order validation:

Density Sine wave

$\rho_0 = 1 + 0.1\sin(2\pi X)\ ,\ u_0 = 1\ ,\ p_0 = 1/\gamma$

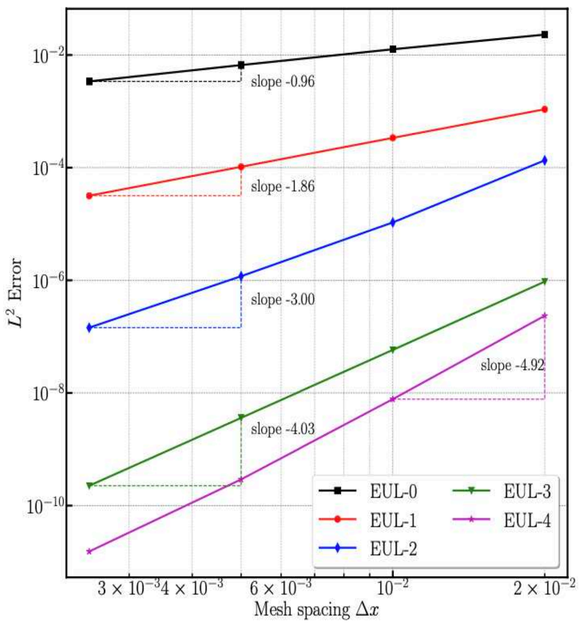

Modified non-linear smooth solution

$X \in [0,1]\ ,\ \rho_0 = 1 + 0.1\sin(2\pi X)\ ,\ u_0 = 0\ ,\ p_0 = \rho_0^\gamma$

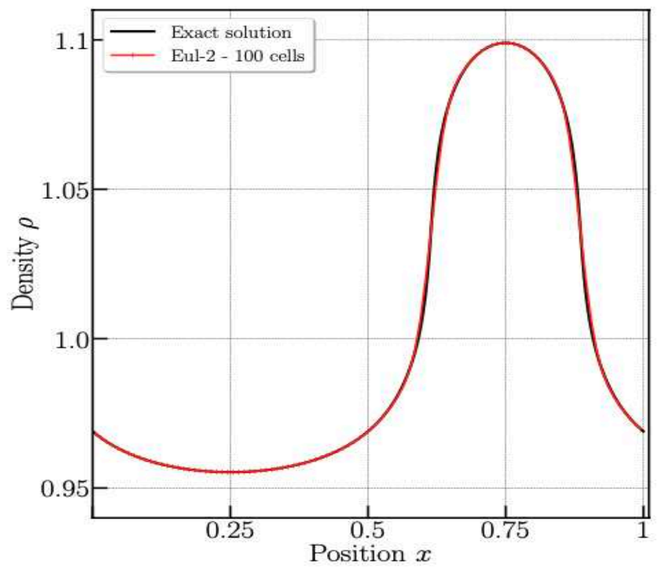

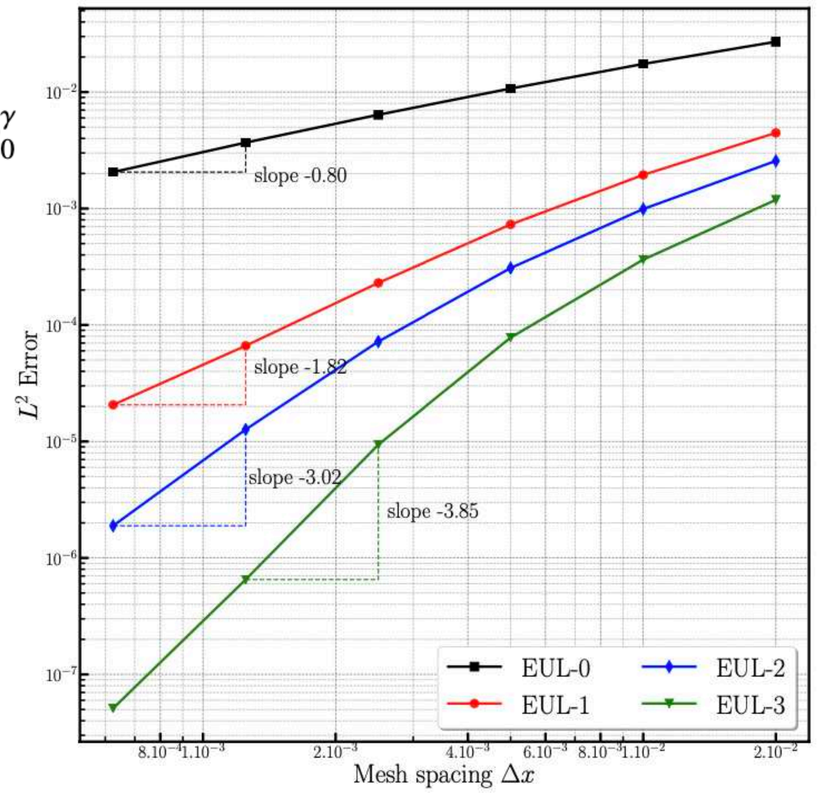

7. S. Clain, S. Diot, and R. Loubère. A high-order finite volume method for systems of conservation laws – multi-dimensional optimal order detection (MOOD). *J. Comput. Phys.*, 230(10):4028 – 4050, 2011.

LeBlanc shock tube - First-order scheme

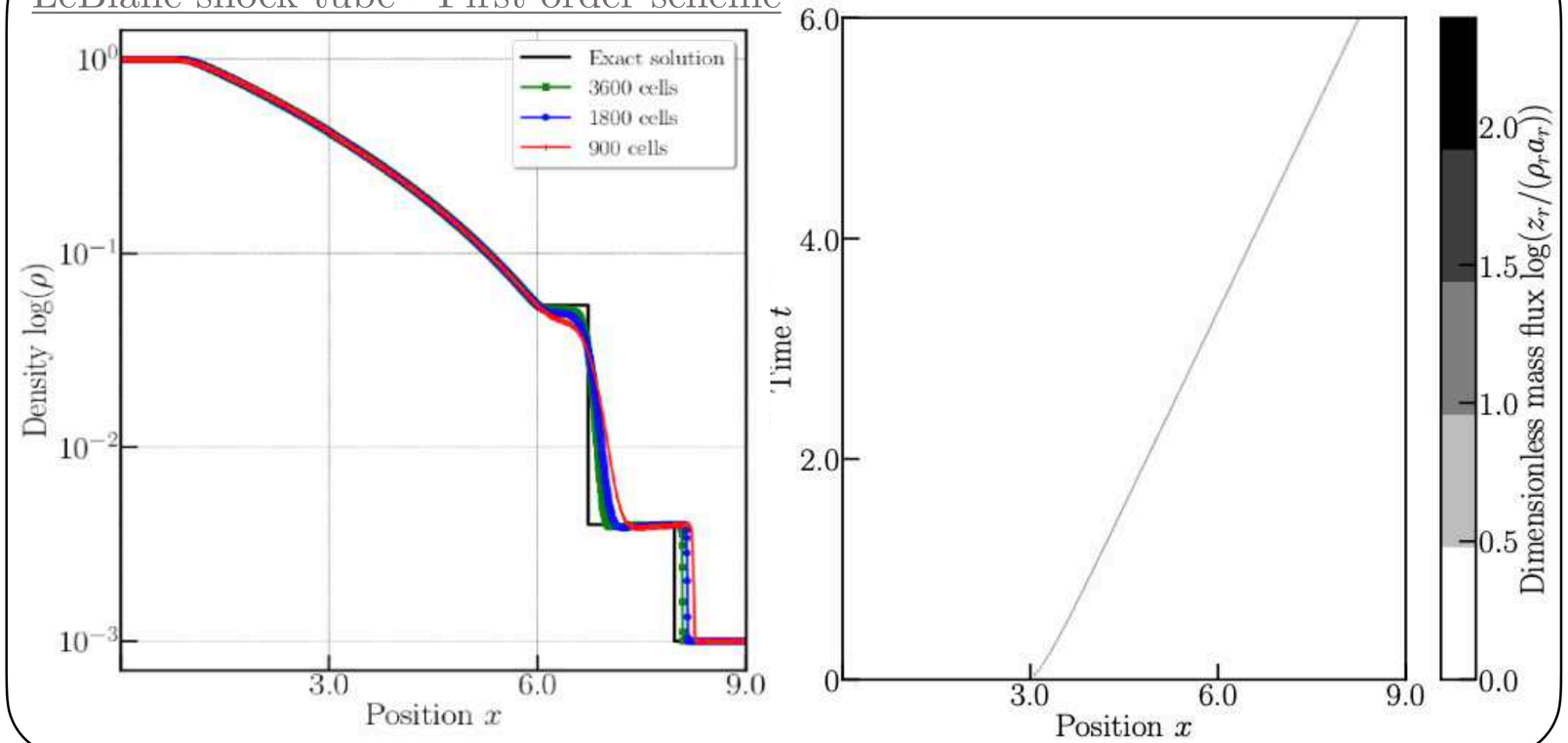

Shu-Osher test case - High-order scheme

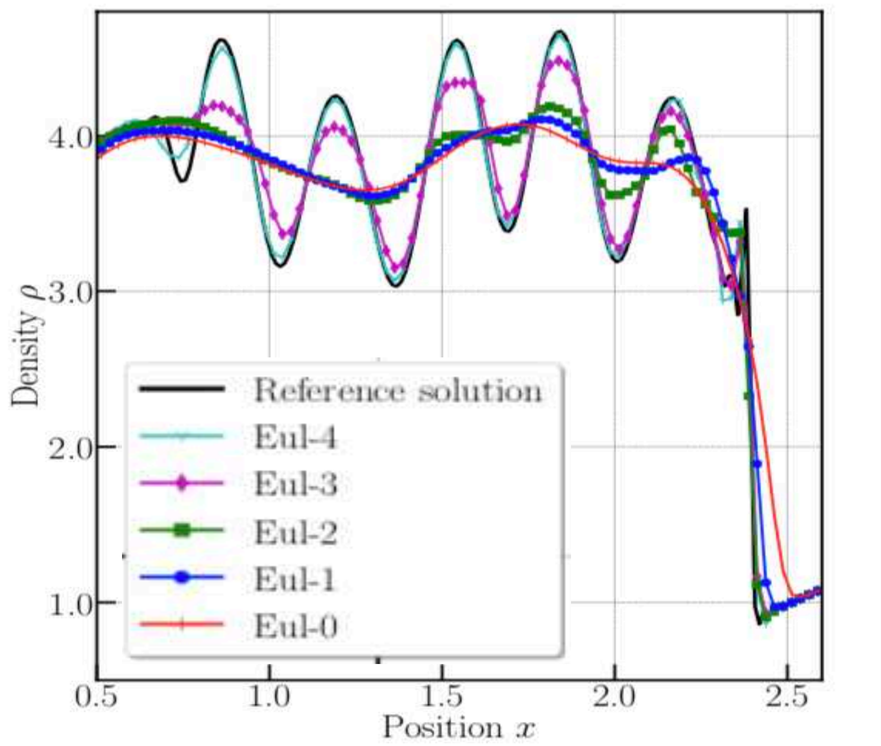

Woodward-Collela blastwave - First-order scheme

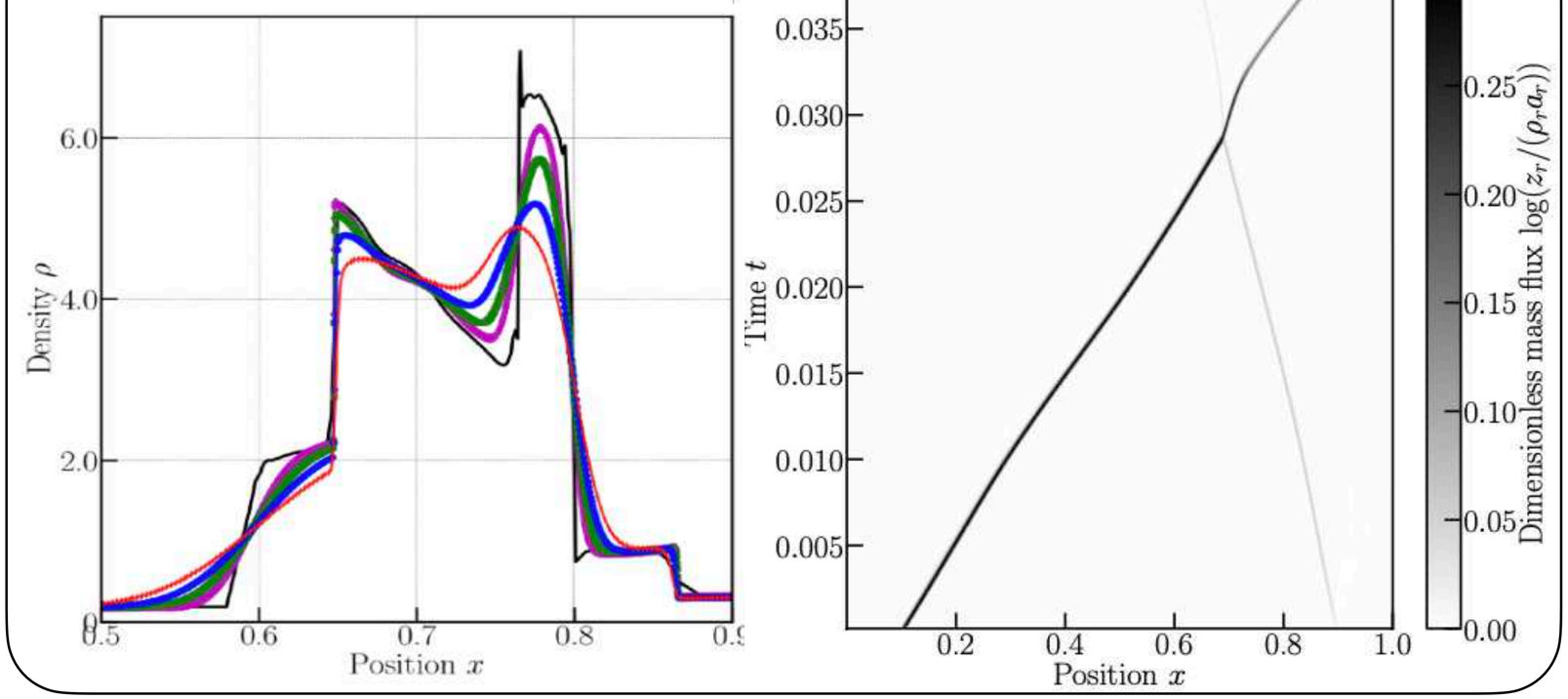

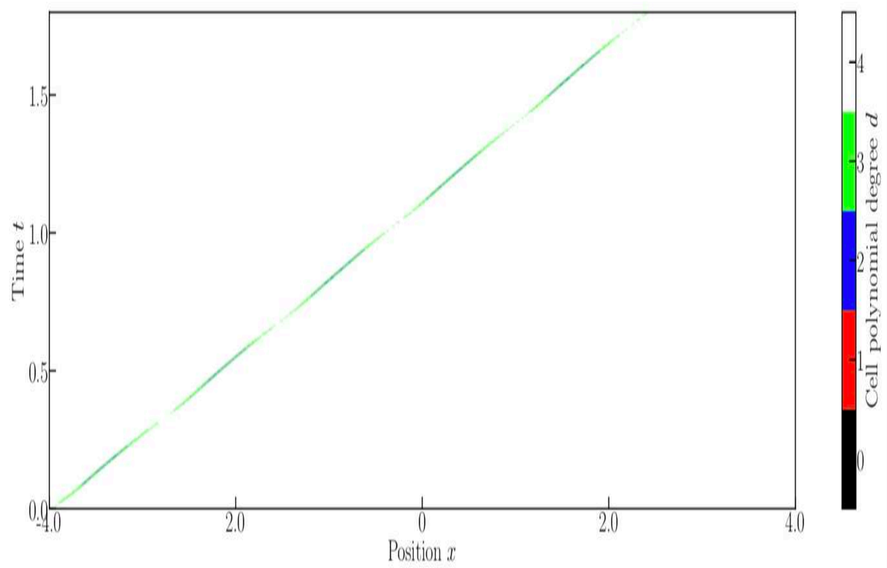

Governing equations :

$$\frac{\partial \mathbf{U}}{\partial t} + \nabla \cdot \mathbb{F}(\mathbf{U}) = \mathbf{0},$$

- Vector of conservative variables : $\mathbf{U} = (\rho, \rho\mathbf{v}, \rho e)^t \in \mathbb{R}^{d+2}$,
- Flux tensor : $\mathbb{F}(\mathbf{U}) \in \mathbb{R}^p \times \mathbb{R}^d$

$$\mathbb{F}(\mathbf{U}) = \begin{pmatrix} \rho\mathbf{v}^t \\ \rho\mathbf{v} \otimes \mathbf{v} + p\mathbb{I}_d \\ \rho e\mathbf{v}^t + p\mathbf{v}^t \end{pmatrix}$$

- $d = 2$ for simplicity.

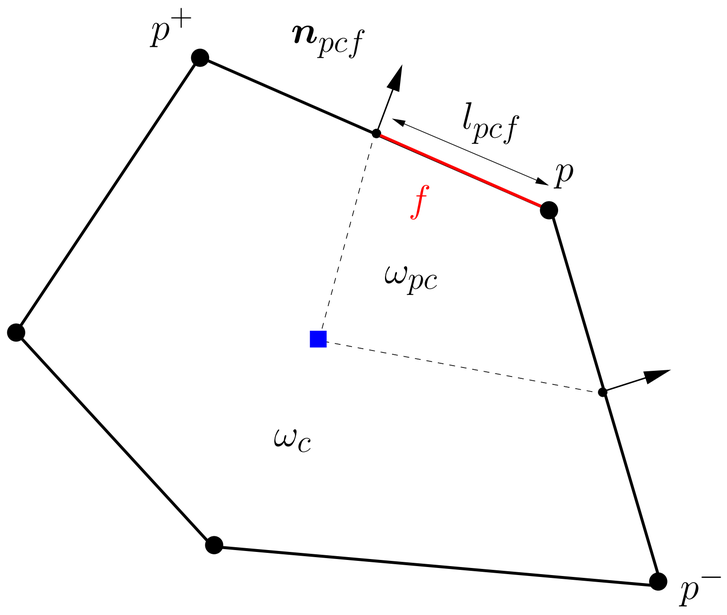

Assumptions :

- Specific internal energy : $\varepsilon = e - \frac{1}{2}\mathbf{v}^2$
- Specific entropy : η
- Convexity assumption : $(\tau, \eta) \to \varepsilon(\tau, \eta)$ strictly convex.
- Gas dynamics entropy inequality : $\frac{\partial \rho\eta}{\partial t} + \nabla \cdot (\rho\eta\mathbf{v}) \geq 0$, and thus

$(\Sigma, \mathbf{Q}) = (-\rho\eta, -\rho\eta\mathbf{v})$.

Geometrical framework :

- $\mathbf{n}$: unit normal to a generic interface,
- $\mathbf{t}$: unit tangent to the interface, such that $(\mathbf{n}, \mathbf{t})$ a direct basis,
- $\mathbf{v} = v_\mathbf{n}\mathbf{n} + v_\mathbf{t}\mathbf{t}, v_\mathbf{n} = \mathbf{v} \cdot \mathbf{n}, v_\mathbf{t} = \mathbf{v} \cdot \mathbf{t}$.

Multi-dimensional generic FV scheme[8]

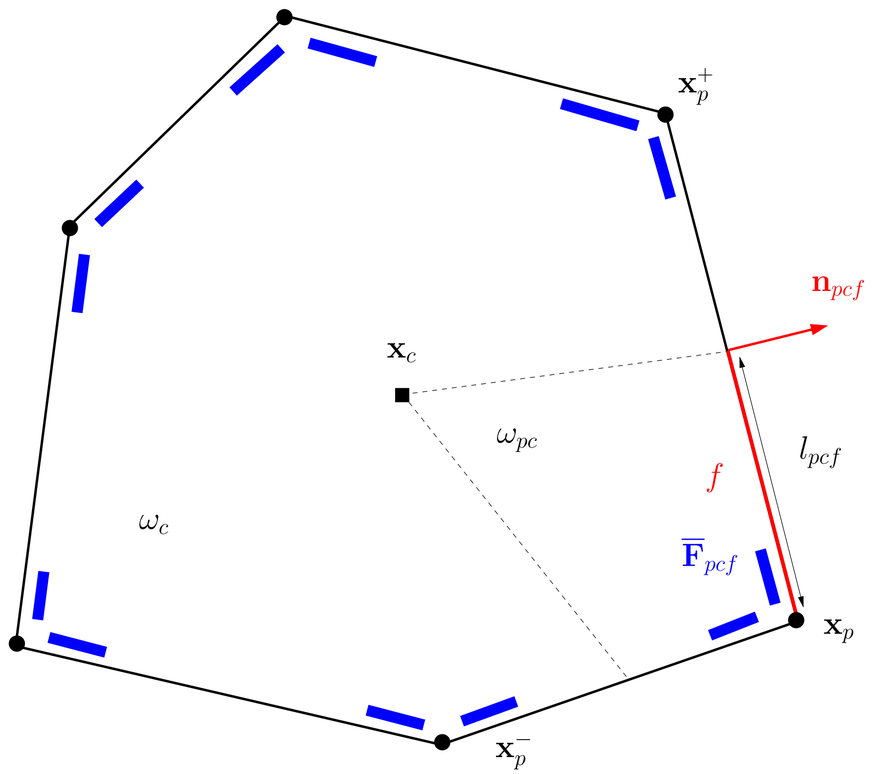

Notations :

- Polygonal tessellation $\cup\, \omega_c$;
- $\mathscr{P}(c)$: List of points of ω_c;
- ω_{pc} : Subcell attached to point p
- $\mathscr{SF}(pc)$: List of subfaces attached to $\partial\omega_c \cap \partial\omega_{pc}$.

Subface-based FV discretization :

$$(1)\ |\omega_c|(\mathbf{U}_c^{n+1} - \mathbf{U}_c^n) + \Delta t \int_{\partial\omega_c \cap \partial\omega_{pc}} \mathbb{F}(\mathbf{U}^n)\mathbf{n} ds = \mathbf{0},$$

$$(2)\ |\omega_c|(\mathbf{U}_c^{n+1} - \mathbf{U}_c^n) + \Delta t \sum_{p\in\mathscr{P}(c)} \sum_{f\in\mathscr{SF}(pc)} l_{pc}\overline{\mathbf{F}}_{pcf} = \mathbf{0},$$

- Subface flux : $\overline{\mathbf{F}}_{pcf} = \mathbb{F}(\mathbf{U}_c^n)\mathbf{n}_{pcf} - \int_{-\infty}^{0} (\mathbf{W}_{pcf}\xi - \mathbf{U}_c^n) d\xi$

8. G. Gallice, A. Chan, R. Loubère and Maire P.-H., Entropy stable and positivity preserving Godunov-type schemes for multidimensional hyperbolic systems on unstructured grid, submitted J. of Comp. Phys.

Subface-based FV discretization :

Non-conservative in the classical sense

$$|\omega_c|(\mathbf{U}_c^{n+1} - \mathbf{U}_c^n) + \Delta t \sum_{p\in\mathscr{P}(c)} \sum_{f\in\mathcal{SF}(pc)} l_{pc}\overline{\mathbf{F}}_{pcf} = \mathbf{0},$$

Properties of subface-based scheme :

- $\mathscr{D}$-preserving property under the time step condition :

$$\Delta t \leq \frac{|\omega_c|}{\sum_{p\in\mathscr{P}(c)} \sum_{f\in\mathcal{SF}(pc)} l_{pcf}\xi_{pcf}^{min}}$$

Remark :

- Conservativity of FV scheme and entropy stability is not guaranteed.

- Retrieve conservativity through **node-based conditions.**

Conservativity of the FV scheme

The FV scheme is **conservative** if and only if :

$$\sum_c |\omega_c|(\mathbf{U}_c^{n+1} - \mathbf{U}_c^n) = \mathbf{0} \leftrightarrow \sum_c \sum_{p\in\mathscr{P}(c)} \sum_{f\in\mathscr{SF}(pc)} l_{pcf}\overline{\mathbf{F}}_{pcf} = \mathbf{0},$$

$$\leftrightarrow \sum_p \sum_{c\in\mathscr{C}(p)} \sum_{f\in\mathscr{SF}(pc)} l_{pcf}\overline{\mathbf{F}}_{pcf} = \mathbf{0},$$

With $\mathscr{C}(p)$: Set of cells sharing point p.

Conservativity and entropy stability assured provided that

$$\sum_{f\in\mathscr{SF}(pc)} l_{pcf}\overline{\mathbf{F}}_{pcf} + l_{pdf}\overline{\mathbf{F}}_{pdf} = \mathbf{0},$$

With d is the neighbouring cell such that $\omega_c \cup \omega_d = f$ and $l_{pcf} = l_{pdf}$.

Remarks :

- Need of an explicit expression of subface flux.

- Construction of 1D RS in the normal direction $\mathbf{n}_{pcf}$

Node-based sufficient condition :

$$\sum_{c\in\mathscr{C}(p)} \sum_{f\in\mathscr{SF}(pc)} l_{pcf}\overline{\mathbf{F}}_{pcf} = \mathbf{0},$$

$$\sum_{f\in\mathscr{SF}(pc)} \sum_{c\in\mathscr{C}(p)} l_{pcf}\overline{\mathbf{F}}_{pcf} = \mathbf{0},$$

With $\mathscr{SF}(p)$: Set of subfaces impinging at point p,

$\mathscr{C}(f)$: Set of cells sharing subface f.

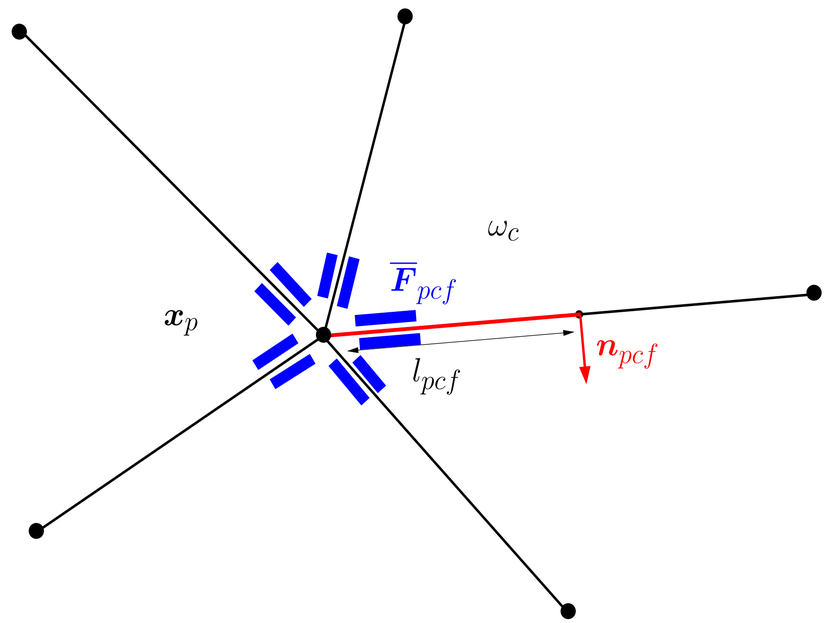

2D Lagrangian gas dynamics

$$\frac{\partial \mathbf{V}}{\partial t} + \frac{\partial \mathbf{G_n}(\mathbf{V})}{\partial m} = \mathbf{0}$$

$$\mathbf{V} = (\tau, v_\mathbf{n}, v_\mathbf{t}, e)^t, \quad \mathbf{G_n} = (-v_\mathbf{n}, p, 0, pv_\mathbf{n})^t$$

Construction of simple Lagrangian solver:

$$\mathbf{W}(\mathbf{V}_l, \mathbf{V}_r, \frac{m}{t}) = \begin{cases} \mathbf{V}_l \text{ if } \frac{m}{t} \leq -\lambda_l, \\ \mathbf{V}_l^\star \text{ if } -\lambda_l < \frac{m}{t} \leq 0, \\ \mathbf{V}_r^\star \text{ if } 0 < \frac{m}{t} \leq \lambda_r, \\ \mathbf{V}_r \text{ if } \lambda_r < \frac{m}{t}. \end{cases}$$

- Intermediate states : $\mathbf{V}_s^\star = (\tau_s^\star, v_{\mathbf{n},s}^\star, v_{\mathbf{t},s}^\star, e_s^\star)^t$,
- Intermediate fluxes : $\overline{\mathbf{G}}_{\mathbf{n},s} = (-v_\mathbf{n}^\star, p_s^\star, 0, p_s^\star v_\mathbf{n}^\star)^t$

Solution of the system :

$$(\mathcal{S}) \begin{cases} \lambda_l(\mathbf{V}_l^\star - \mathbf{V}_l) + \overline{\mathbf{G}}_\mathbf{n}^- - \mathbf{G}_{\mathbf{n},l} = 0, \\ -\lambda_r(\mathbf{V}_r - \mathbf{V}_r^\star) + \overline{\mathbf{G}}_\mathbf{n}^+ - \mathbf{G}_{\mathbf{n},r} = 0, \end{cases}$$

Left and right flux :

$$\overline{\mathbf{G}}_n^- = \mathbf{G}_{n,l} - \sum_{k=1}^{m} \lambda_k(\mathbf{V}_{k+1} - \mathbf{V}_k),$$

$$\overline{\mathbf{G}}_n^+ = \mathbf{G}_{n,r} - \sum_{k=1}^{m} \lambda_k(\mathbf{V}_{k+1} - \mathbf{V}_k),$$

$\mathbf{W}$ induces a conservative Godunov-type FV scheme if

$$\overline{\mathbf{G}}_\mathbf{n}^+ - \overline{\mathbf{G}}_\mathbf{n}^- = -\sum_{k=1}^{m} \lambda_k(\mathbf{V}_{k+1} - \mathbf{V}_k) + \mathbf{G}_{\mathbf{n},r} - \mathbf{G}_{\mathbf{n},l} = \mathbf{0},$$

The usual 1D interface flux is simply given by $\overline{\mathbf{G}}_\mathbf{n} = \frac{1}{2}(\overline{\mathbf{G}}_n^- + \overline{\mathbf{G}}_\mathbf{n}^+)$, and writes $\overline{\mathbf{G}}_\mathbf{n} = \frac{1}{2}\sum_{k=1}^{m} |\lambda_k|(\mathbf{V}_{k+1} - \mathbf{V}_k)$.

($\mathcal{S}$) develops into :

$$(\mathcal{S}_l)\begin{cases} \lambda_l(\tau_l^\star - \tau_l) - (v_{\mathbf{n}}^\star - v_{\mathbf{n},l}) = 0, \\ \lambda_l(v_{\mathbf{n}}^\star - v_{\mathbf{n},l}) - (p_l^\star - p_l) = 0, \\ \lambda_l(v_{\mathbf{t}}^\star - v_{\mathbf{t},l}) = 0, \\ \lambda_l(e_l^\star - e_l) - (p_l^\star v_{\mathbf{n}}^\star - p_l v_{\mathbf{n},l}) = 0, \end{cases} \quad (\mathcal{S}_r)\begin{cases} \lambda_r(\tau_r^\star - \tau_r) + (v_{\mathbf{n}}^\star - v_{\mathbf{n},r}) = 0, \\ \lambda_r(v_{\mathbf{n}}^\star - v_{\mathbf{n},r}) - (p_r^\star - p_r) = 0, \\ \lambda_r(v_{\mathbf{t}}^\star - v_{\mathbf{t},r}) = 0, \\ \lambda_r(e_r^\star - e_r) - (p_r^\star v_{\mathbf{n}}^\star - p_r v_{\mathbf{n},r}) = 0, \end{cases}$$

9 unknowns for 8 equations → $v_{\mathbf{n}}^\star$ is viewed as a parameter.

Consistency of Lagrangian solver $(\mathcal{S}_l) + (\mathcal{S}_r)$:

$$\overline{\mathbf{G}}_{\mathbf{n}}^{+} - \overline{\mathbf{G}}_{\mathbf{n}}^{-} = \lambda_l(\mathbf{V}_l^\star - \mathbf{V}_l) - \lambda_r(\mathbf{V}_r - \mathbf{V}_r^\star) + \mathbf{G}_{\mathbf{n},r} - \mathbf{G}_{\mathbf{n},l} \quad (1)$$

Combine second equation of $(\mathcal{S}_l)$ and $(\mathcal{S}_r)$:

$$(2)\ p_r^\star - p_l^\star = (\lambda_l + \lambda_r)(v_{\mathbf{n}}^\star - \overline{v}_{\mathbf{n}})$$

$$\text{where } \overline{v}_{\mathbf{n}} = \frac{\lambda_l v_{\mathbf{n},l} + \lambda_r v_{\mathbf{n},r}}{\lambda_l + \lambda_r} - \frac{(p_r - p_l)}{\lambda_l + \lambda_r}$$

- If $v_{\mathbf{n}}^\star = \overline{v}_{\mathbf{n}}$: Conservative Godunov-type FV scheme.
- If $v_{\mathbf{n}}^\star \neq \overline{v}_{\mathbf{n}}$: $v_{\mathbf{n}}^\star$ is a parameter, $p_r^\star \neq p_l^\star$, non-conservative Godunov-type FV scheme.

  → call upon **node-based conservation condition.**

Generic node-based conservation condition $\sum_{f\in\mathcal{SF}(pc)}\sum_{c\in\mathcal{C}(p)} l_{pcf}\overline{\mathbf{F}}_{pcf}=\mathbf{0}$:

Substitute Lagrangian flux in $\overline{\mathbf{F}}_{pcf}$:

$$-\left[\sum_{k=1}^{m}\lambda_k(\mathbf{V}_{k+1}-\mathbf{V}_k)\right]_{c,d}+\mathbf{G}_{\mathbf{n},r}-\mathbf{G}_{\mathbf{n},l}$$

$$=\overline{\mathbf{G}}_{\mathbf{n}}^{+}-\overline{\mathbf{G}}_{\mathbf{n}}^{-}=(p_r^\star-p_l^\star)\begin{pmatrix}0\\1\\0\\v_{\mathbf{n}}^\star\end{pmatrix}.$$

Node-based conservation condition writes :

$$\sum_{f\in\mathcal{SF}(p)} l_{pcf}(p_r^\star-p_l^\star)\begin{pmatrix}0\\1\\0\\v_{\mathbf{n}}^\star\end{pmatrix}=\mathbf{0}$$

We prescribe $v_{\mathbf{n}}^\star=\mathbf{v}_p\cdot\mathbf{n}$,

$\mathbf{v}_p$ is the nodal velocity.

Node-based conservation boils down to **nodal solver** :

$$\sum_{f\in\mathcal{SF}(p)} l_{pcf}(\lambda_l+\lambda_r)(\mathbf{n}_{pcf}\otimes\mathbf{n}_{pcf})\mathbf{v}_p=\sum_{f\in\mathcal{SF}(p)} l_{pcf}(\lambda_l+\lambda_r)\overline{v}_{\mathbf{n},pcf}\mathbf{n}_{pcf},$$

$$\text{where } \overline{v}_{\mathbf{n}_{pcf}}=\frac{\lambda_l v_{\mathbf{n}_{pcf,c}}+\lambda_r v_{\mathbf{n}_{pcf,d}}}{\lambda_l+\lambda_r}-\frac{p_r-p_l}{\lambda_l+\lambda_r}.$$

The system always admits a unique solution providing an approximation of the nodal velocity.

2D Eulerian gas dynamics

$$\frac{\partial \mathbf{U}}{\partial t} + \frac{\partial \mathbf{F_n}(\mathbf{U})}{\partial x_\mathbf{n}} = \mathbf{0}$$

$$\mathbf{U} = (\rho, \rho v_\mathbf{n}, \rho v_\mathbf{t}, \rho e)^t,$$

$$\mathbf{F_n} = (\rho v_\mathbf{n}, \rho v_\mathbf{n}^2 + p, \rho v_\mathbf{n} v_\mathbf{t}, \rho v_\mathbf{n} e + p v_\mathbf{n})^t$$

Eigenvalues : $v_\mathbf{n} - a, v_\mathbf{n}\ ,\ v_\mathbf{n}\ ,\ v_\mathbf{n} + a$

Entropy inequality : $\frac{\partial \rho\eta}{\partial t} + \frac{\partial}{\partial x}(\rho\eta v_\mathbf{n}) \geq 0.$

Subface Riemann problem :

$$\frac{\partial \mathbf{U}}{\partial t} + \frac{\partial \mathbf{F_n}}{\partial x_\mathbf{n}} = \mathbf{0}, \text{ where } \mathbf{F_n} = \mathbb{F}(\mathbf{U})\mathbf{n}$$

$$\mathbf{U}(x_\mathbf{n}, 0) \begin{cases} \mathbf{U}_l \text{ if } x_\mathbf{n} < 0, \\ \mathbf{U}_r \text{ if } x_\mathbf{n} \geq 0. \end{cases}$$

Eulerian RP with respect to the 1D Eulerian coordinate $x_\mathbf{n} = \mathbf{x} \cdot \mathbf{n}$.

Construction of **simple Eulerian solver :**

$$\mathbf{W}^{eul}(\mathbf{U}_l, \mathbf{U}_r, \frac{x_\mathbf{n}}{t}) = \begin{cases} \mathbf{U}_l & \text{if} \quad \frac{x_n}{t} \leq \Lambda_l \\ \mathbf{U}_l^\star & \text{if} \quad \Lambda_l < \frac{x_n}{t} \leq \Lambda_0 \\ \mathbf{U}_r^\star & \text{if} \quad \Lambda_0 < \frac{x_n}{t} \leq \Lambda_r \\ \mathbf{U}_r & \text{if} \quad \Lambda_r \leq \frac{x_n}{t} \end{cases}$$

Eulerian wave speeds :

$$\begin{cases} \Lambda_l = v_{\mathbf{n},l} - \lambda_l \tau_l = v_\mathbf{n}^\star - \lambda_l \tau_l^\star, \\ \Lambda_0 = v_\mathbf{n}^\star, \\ \Lambda_r = v_{\mathbf{n},r} + \lambda_r \tau_r = v_\mathbf{n}^\star - \lambda_r \tau_r^\star, \end{cases}$$

By means of Lagrange-to-Euler mapping $\mathbf{V} \rightarrow \mathbf{U}(\mathbf{V})$:

- Intermediate states : $\mathbf{U}_s^\star = (\rho_s^\star, \rho_s^\star v_{\mathbf{n},s}^\star, \rho_s^\star v_{\mathbf{t},s}^\star, \rho_s^\star e_s^\star)^t$.

Relation between Lagrangian and Eulerian fluxes :

Lagrangian left & right fluxes

$$\overline{\mathbf{G}}_n^- = \mathbf{G}_{n,l} - \sum_{k=1}^{m} \lambda_k(\mathbf{V}_{k+1} - \mathbf{V}_k),$$

$$\overline{\mathbf{G}}_n^+ = \mathbf{G}_{n,r} - \sum_{k=1}^{m} \lambda_k(\mathbf{V}_{k+1} - \mathbf{V}_k),$$

$$\overline{\mathbf{G}}_n^+ - \overline{\mathbf{G}}_n^- = -\sum_{k=1}^{m} \lambda_k(\mathbf{V}_{k+1} - \mathbf{V}_k) + \mathbf{G}_n(\mathbf{V}_r) - \mathbf{G}_n(\mathbf{V}_l)$$

Eulerian left & right fluxes

$$(1)\ \overline{\mathbf{F}}_\mathbf{n}^+ - \overline{\mathbf{F}}_\mathbf{n}^- = -\sum_{k=1}^{m} \Lambda_k(\mathbf{U}_{k+1} - \mathbf{U}_k) + \mathbf{F}_n(\mathbf{U}_r) - \mathbf{F}_n(\mathbf{U}_l)$$

Substitute expression of eulerian wave speeds $\Lambda_k = v_{n,k} + \lambda_k \tau_k$ and

using Lagrange-to-Euler mapping :

$$(2)\ \overline{\mathbf{F}}_\mathbf{n}^+ - \overline{\mathbf{F}}_\mathbf{n}^- = -\sum_{k=1}^{m} \lambda_k(\mathbf{V}_{k+1} - \mathbf{V}_k) + \mathbf{G}_{n,r} - \mathbf{G}_{n,l}$$

Fundamental formula :

$$-\sum_{k=1}^{m} \Lambda_k(\mathbf{U}_{k+1} - \mathbf{U}_k) + \mathbf{F}_n(\mathbf{U}_r) - \mathbf{F}_n(\mathbf{U}_l) = -\sum_{k=1}^{m} \lambda_k(\mathbf{V}_{k+1} - \mathbf{V}_k) + \mathbf{G}_n(\mathbf{V}_r) - \mathbf{G}_n(\mathbf{V}_l),$$

$$\overline{\mathbf{F}}_n^+ - \overline{\mathbf{F}}_n^- = \overline{\mathbf{G}}_n^+ - \overline{\mathbf{G}}_n^-$$

Summary of the subface-based FV scheme:

1. Subface-based FV scheme :

$$\mathbf{U}_c^{n+1} - \mathbf{U}_c^n + \frac{\Delta t}{|\omega_c|} \sum_{p \in \mathscr{P}(c)} \sum_{f \in \mathscr{SF}(pc)} l_{pcf} \overline{\mathbf{F}}_{pcf} = \mathbf{0},$$

2. Lagrange-to-Euler mapping :

$$-\sum_{k=1}^{m} \Lambda_k (\mathbf{U}_{k+1} + \mathbf{U}_k) - \mathbf{F}_{n,r} - \mathbf{F}_{n,l} = -\sum_{k=1}^{m} \lambda_k (\mathbf{V}_{k+1} - \mathbf{V}_k) + \mathbf{G}_{n,r} - \mathbf{G}_{n,l}$$

3. Subface flux $\overline{\mathbf{F}}_{pcf} = \mathbf{F}^-_{pcf}$ writes :

$$\overline{\mathbf{F}}_{pcf} = \frac{1}{2}[\mathbf{F}_{n,pcf}(\mathbf{U_c}) + \mathbf{F}_{n,pcf}(\mathbf{U}_d)] - \frac{1}{2}\left[\sum_{k=1}^{m} |\Lambda_k| (\mathbf{U}_{k+1} - \mathbf{U}_k)\right]_{c,d}$$

$$-\frac{1}{2}(\lambda_l + \lambda_r)[\mathbf{v}_p \cdot \mathbf{n}_{pcf} - \overline{v}_{\mathbf{n},pcf}] \begin{pmatrix} 0 \\ 1 \\ 0 \\ \mathbf{V}_p \cdot \mathbf{n}_{pcf} \end{pmatrix}.$$

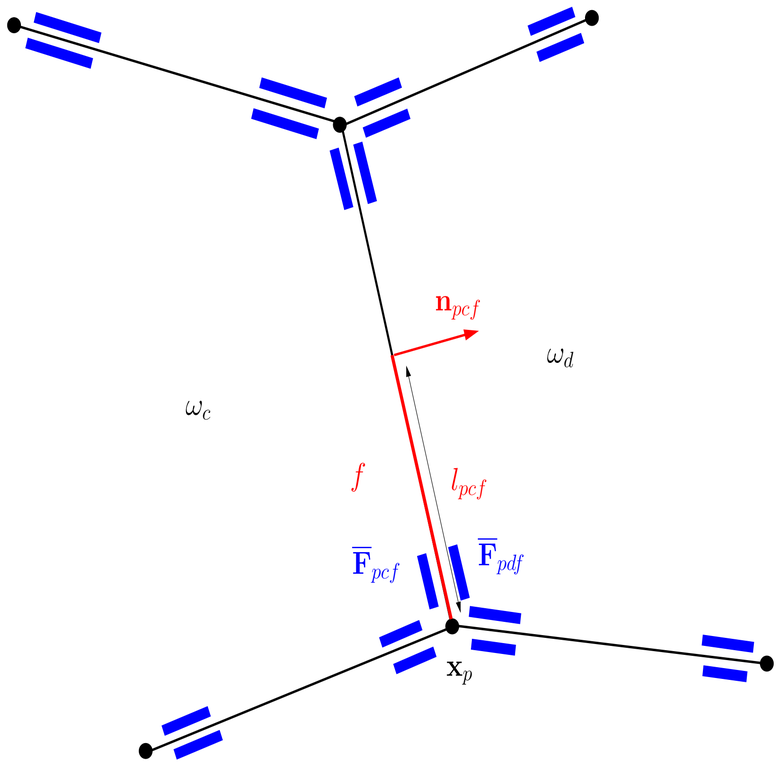

The multi-dimensional numerical flux corresponds to the

classical one-dimensional numerical flux + nodal contribution from the node velocity $\mathbf{v}_p$

Classical FV scheme : Two-point scheme

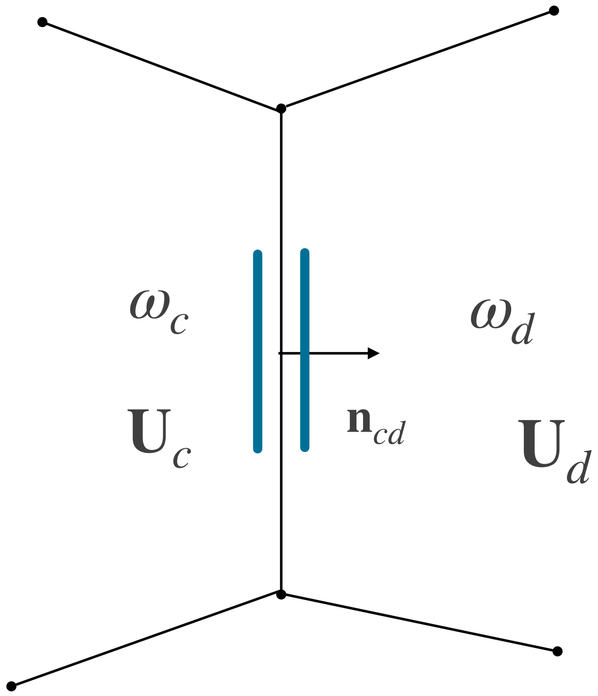

Stencil

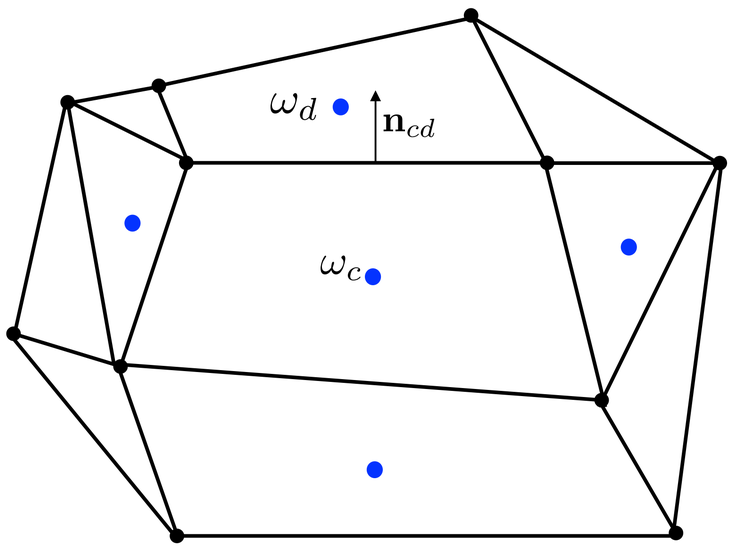

Subface-based FV scheme - Multi-point scheme

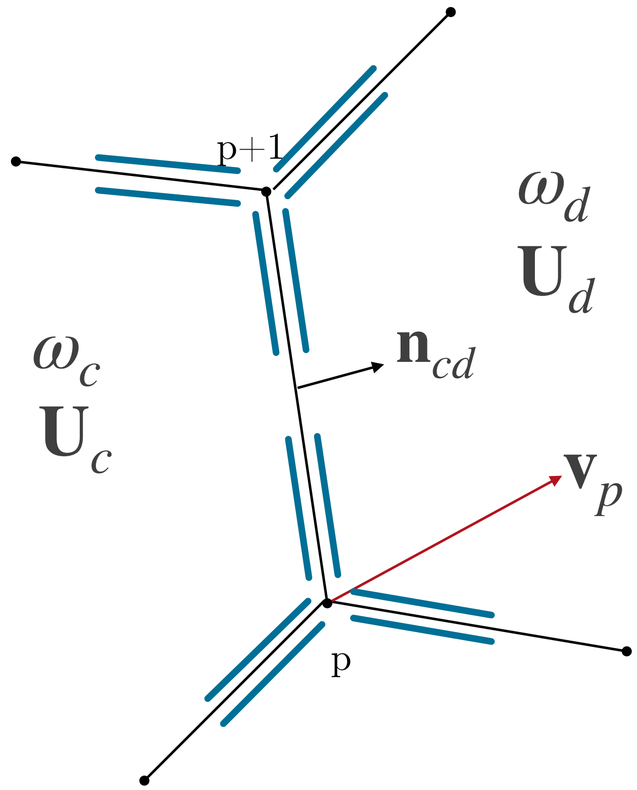

Stencil

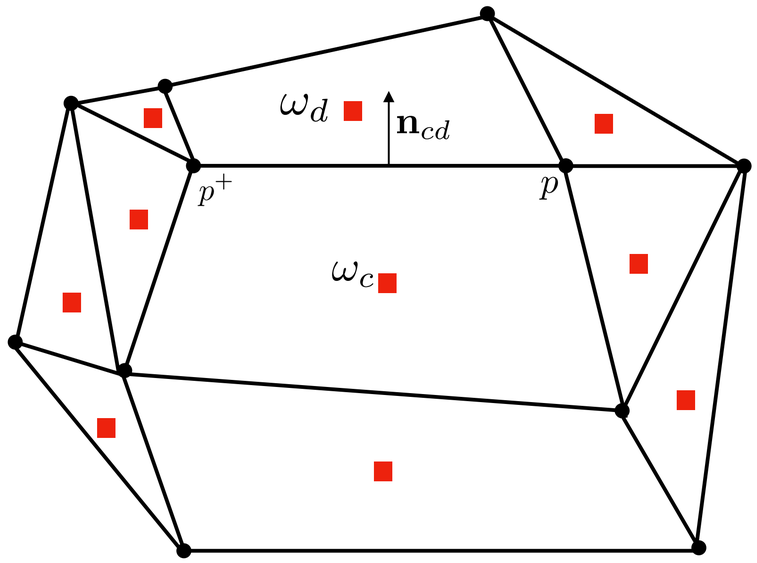

Comparison of first-order two-point solver and multi-point solver.

Odd-even decoupling

Two-point solver

Multi-point solver

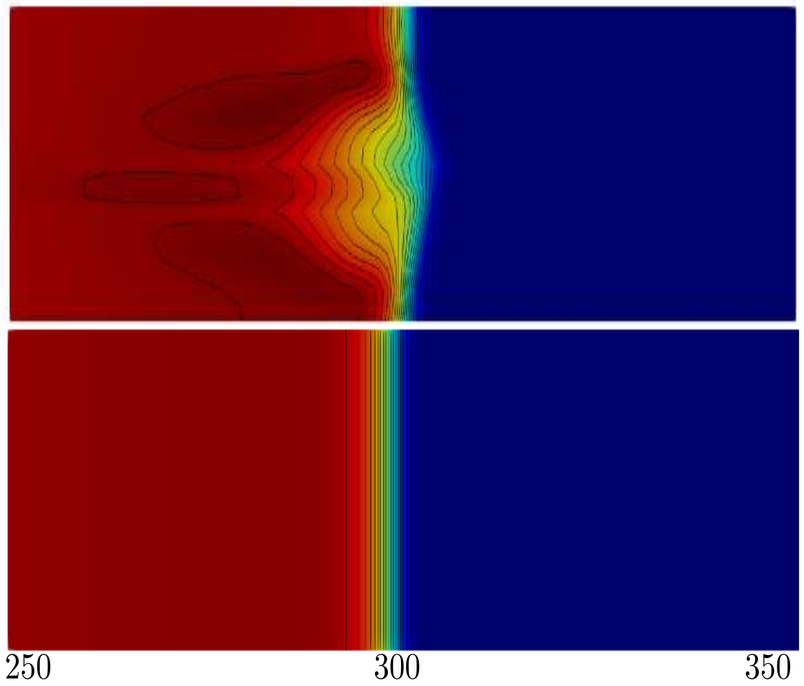

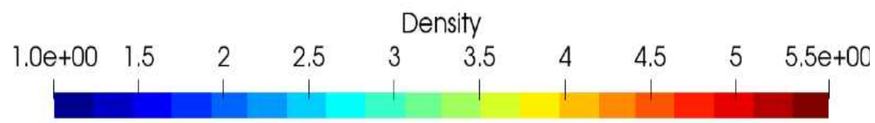

Deviation ε_0 en fonction de la position de choc X_s

$$\varepsilon_0 = max_{i,j}(|\rho_{i,j} - \overline{\rho_i}|),$$

$$\overline{\rho_i} = \frac{1}{J}\sum_{j=1}^{J} \rho_{i,j}$$

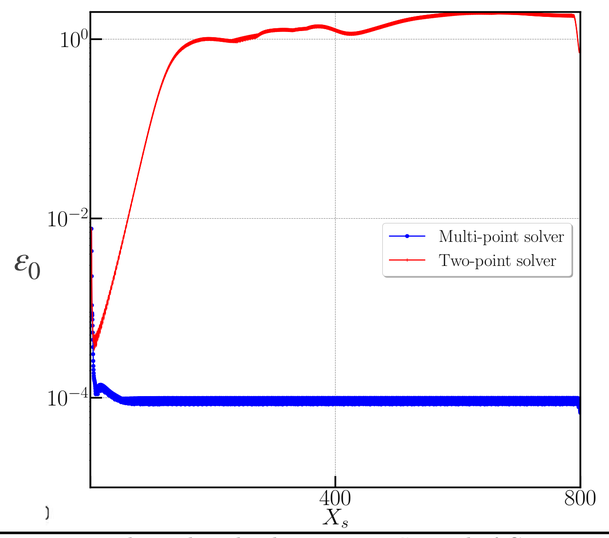

Modified Odd-even decoupling[11]

Two-point solver

Multi-point solver

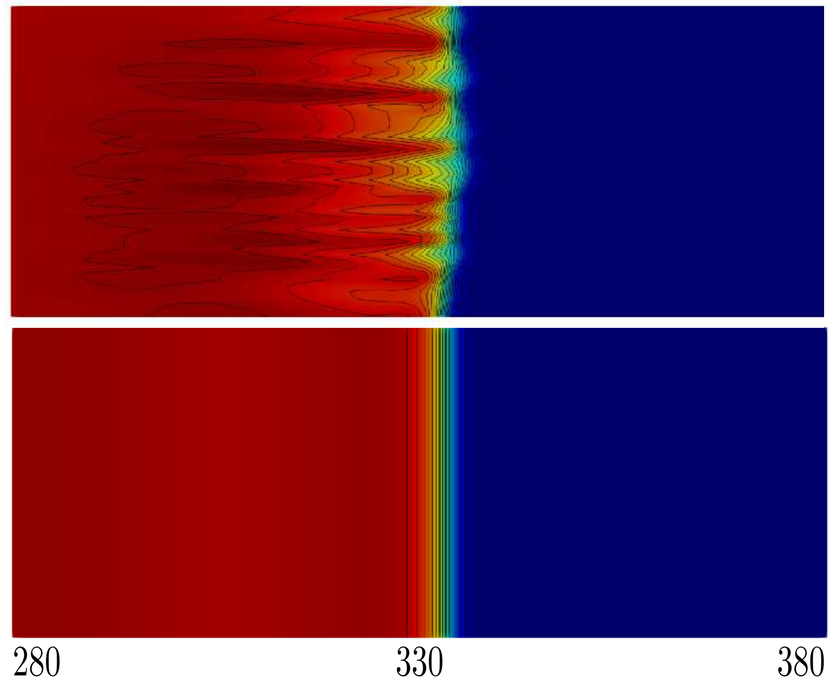

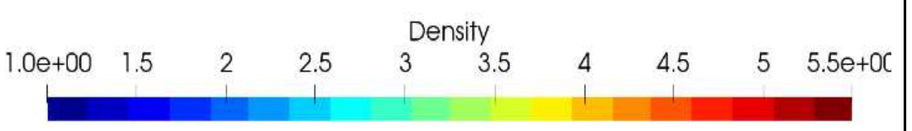

Deviation ε_0 en fonction de la position de choc X_s

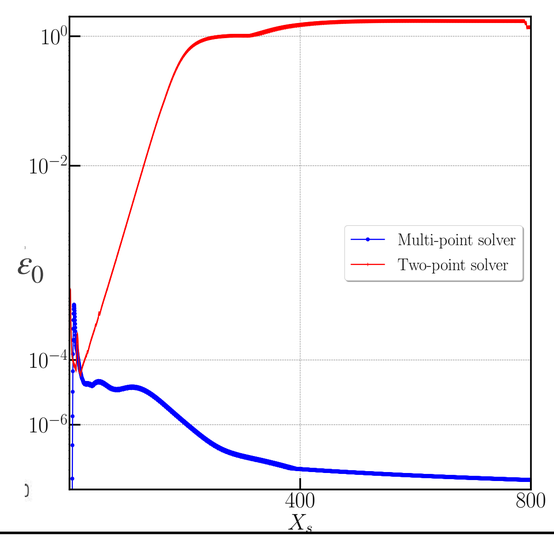

11. A.V. Rodionov, artificial viscosity Godunov-type schemes to cure the carbuncle phenomenon, Journal of Computational Physics(345):208-329, 2017

Comparison of first-order two-point solver and multi-point solver.

Mach 20 flow over half-cylinder

Two-point solver

Multi-point solver

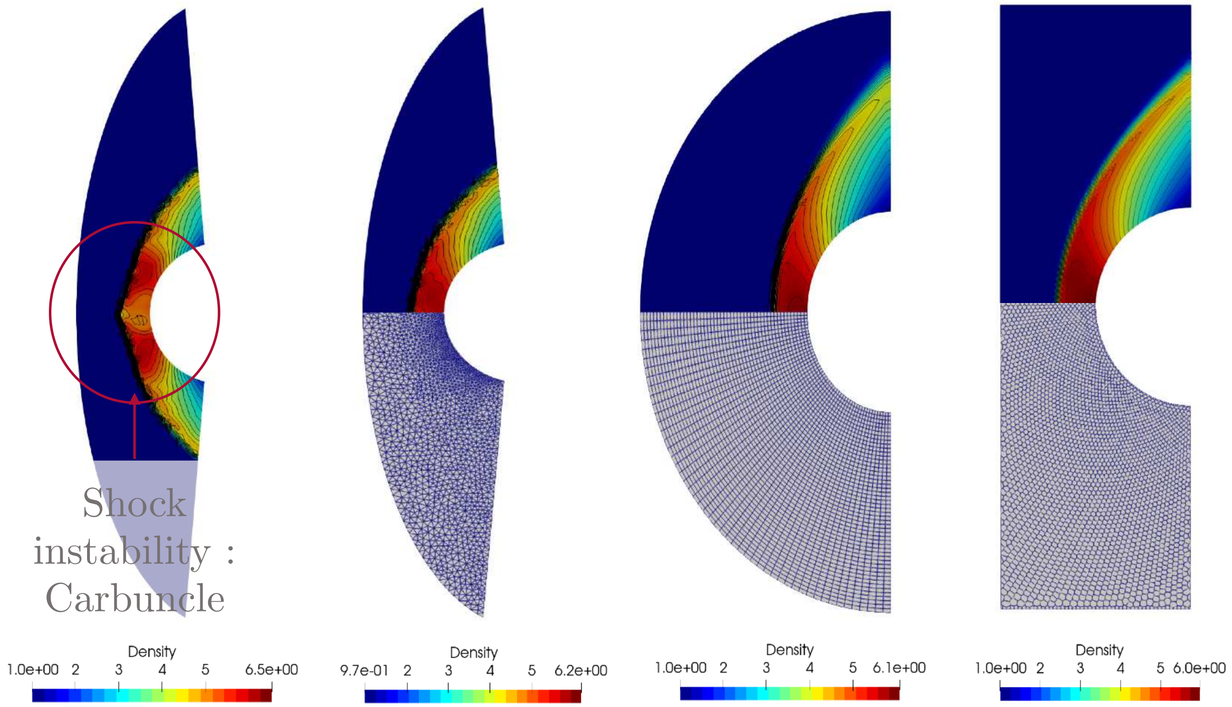

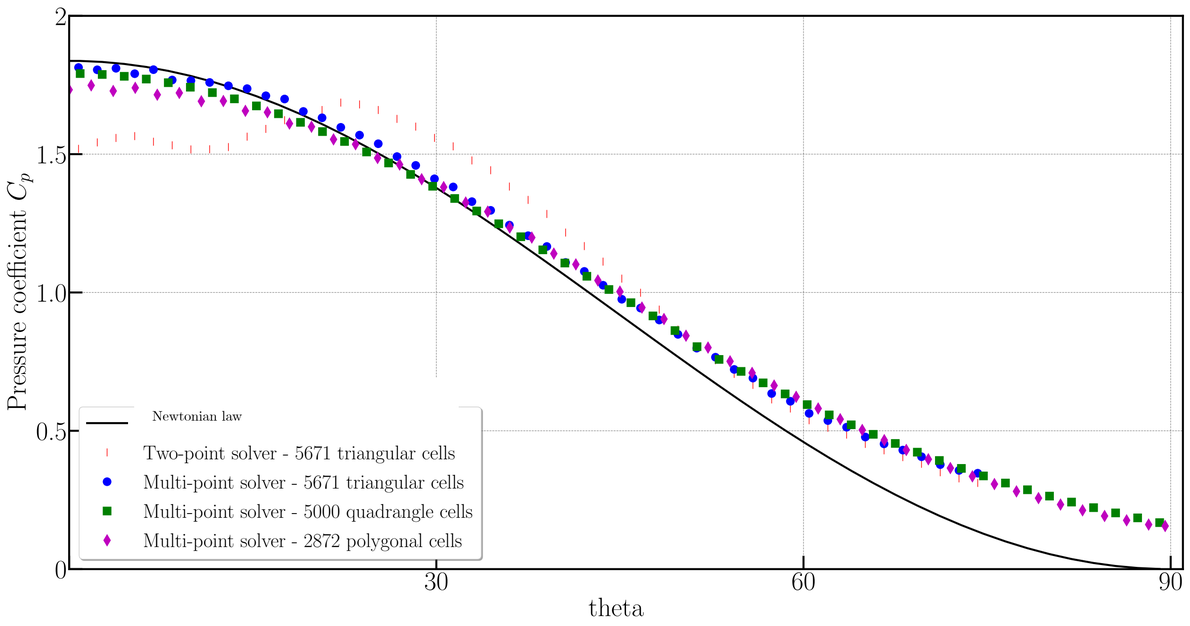

Noh test case on a polar grid

Two-point solver

Multi-point solver

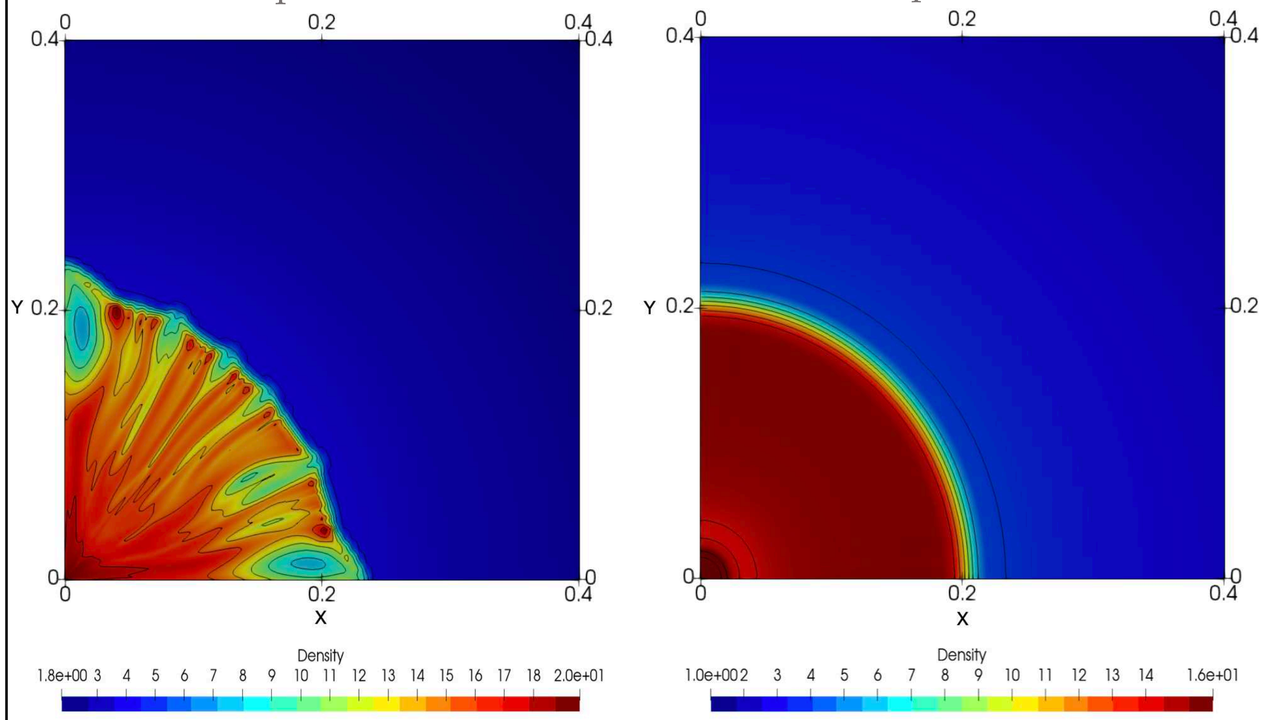

Two-point solver scatter plot

Multi-point solver scatter plot - Symmetrical solution

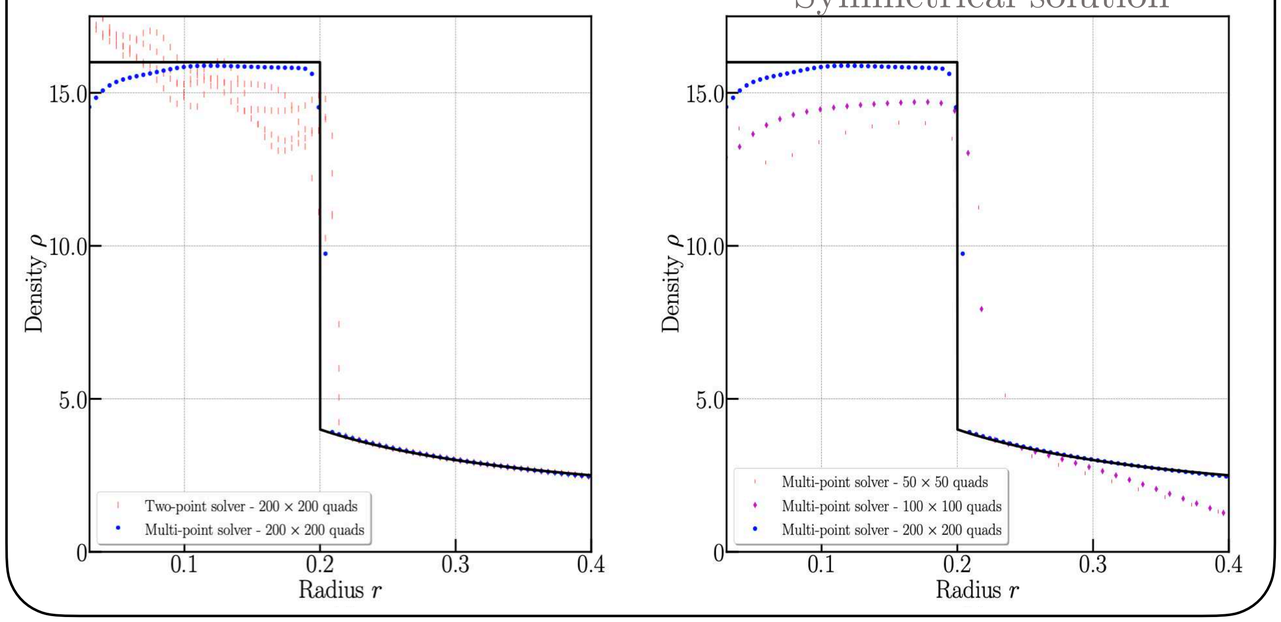

Comparison of first-order two-point solver and multi-point solver.

Sedov test case[12]

Cartesian grid

Two-point solver

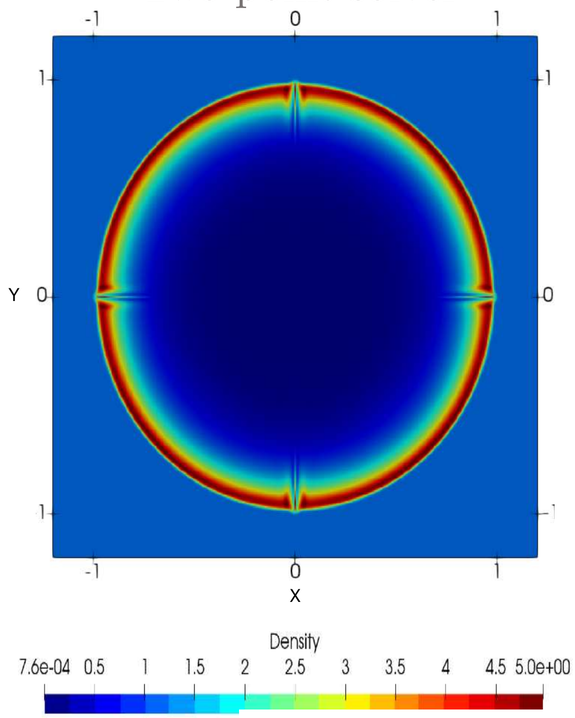

Multi-point solver

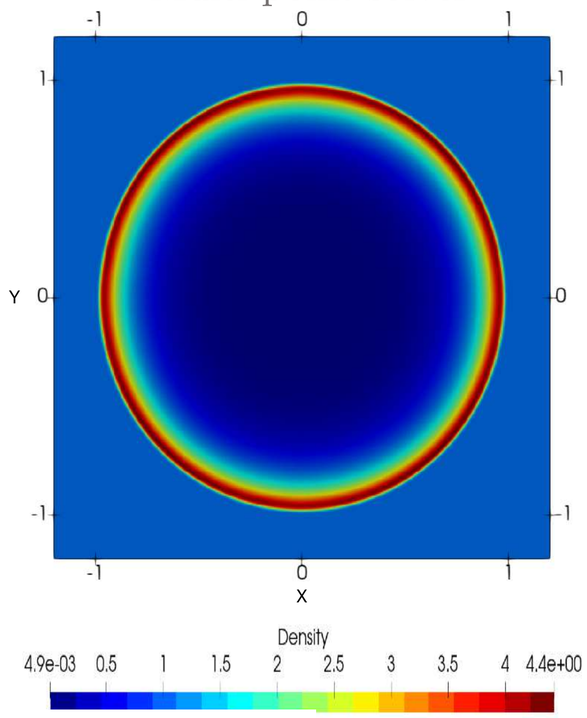

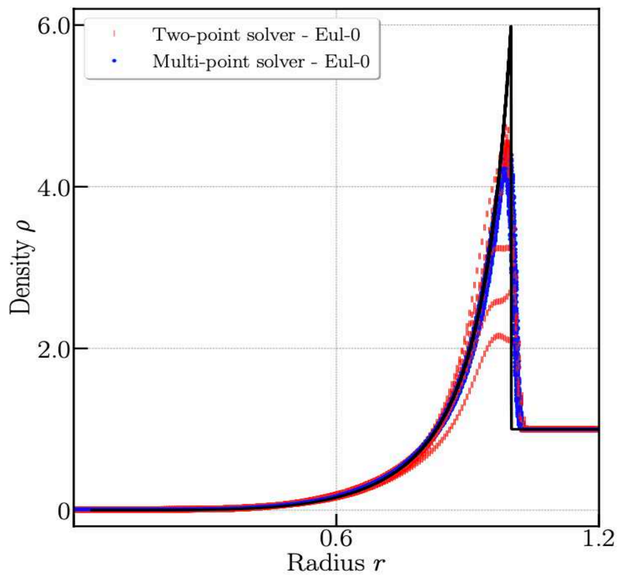

Irregular cartesian grid

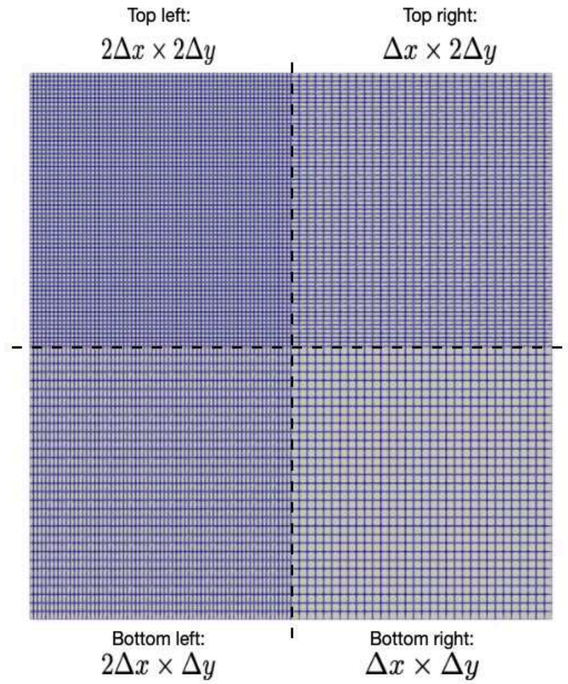

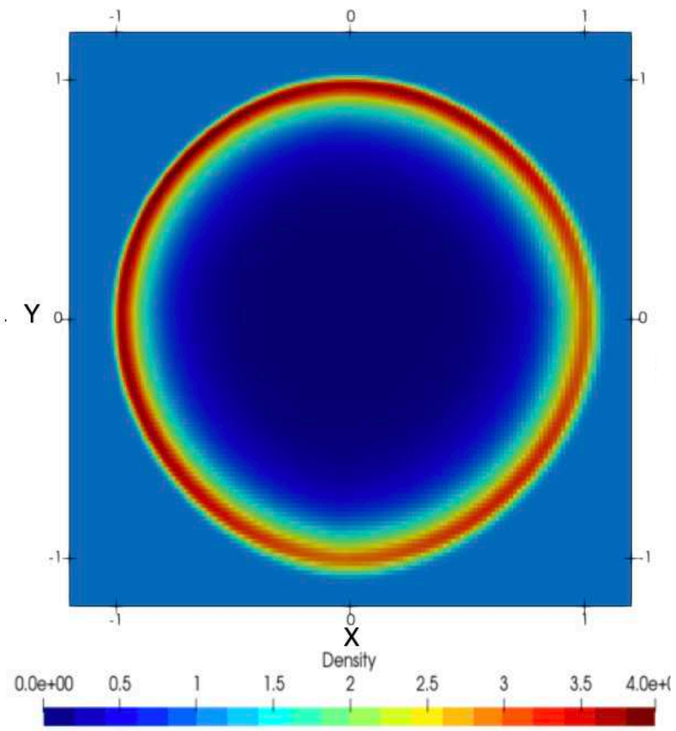

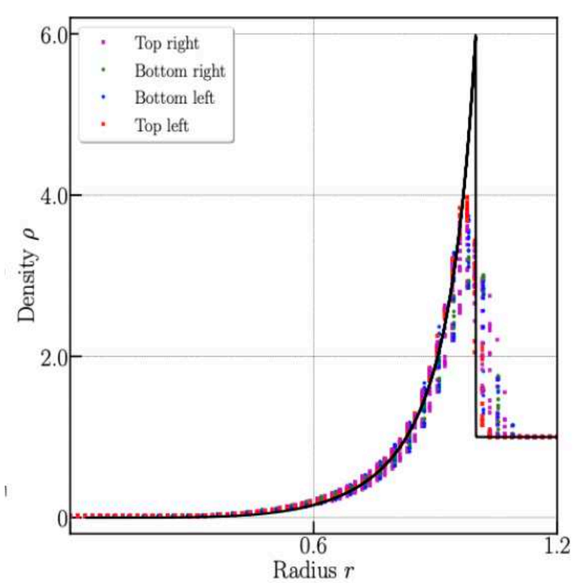

12. N. Fleischmann, S. Adami, N. Adams, A shock-stable modification of the HLLC Riemann solver with reduced numerical dissipation, Journal of Computational Physics(423), 2020.

Second order extension for both two-point and multi-point solver

Isentropic vortex

		Two-point scheme		Multi-point scheme	
	$N \times N$	L^2 error	L^2 order	L^2 error	L^2 order
Eul-0	25×25	$3.2265E-03$	–	$2.3836E-03$	–
	50×50	$1.5660E-03$	1.04	$1.1269E-03$	1.08
	100×100	$7.8289E-04$	1.00	$5.5048E-04$	1.03
	200×200	$3.9078E-04$	1.00	$2.7316E-04$	1.01
	400×400	$1.9656E-04$	0.99	$1.3518E-04$	1.01
		Expected	1	Expected	1
Eul-1	25×25	$1.2312E-05$	–	$3.2875E-05$	–
	50×50	$2.9202E-06$	2.07	$1.9563E-06$	1.79
	100×100	$6.9651E-07$	2.07	$2.8055E-06$	1.75
	200×200	$1.7560E-07$	1.98	$7.7364E-07$	1.86
	400×400	$4.2756E-08$	2.04	$2.0124E-07$	1.95
		Expected	2	Expected	2

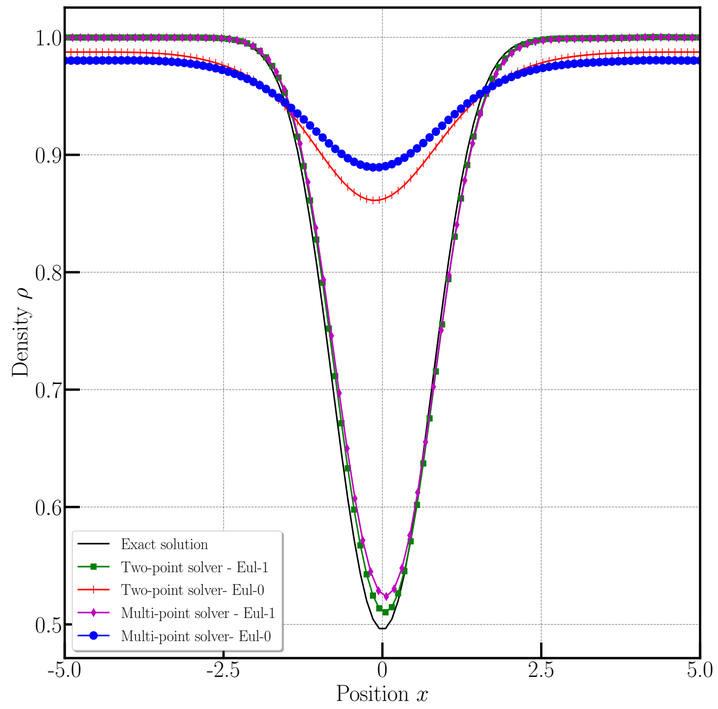

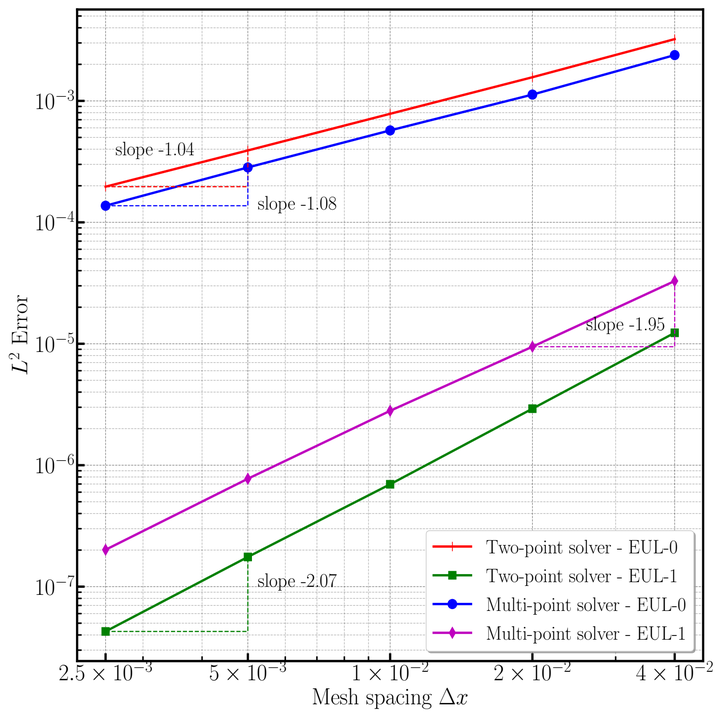

Comparison of first-order and second-order two-point solver and multi-point solver.

Mach 3 flow over forward-facing step[13]

Two-point solver Eul-0

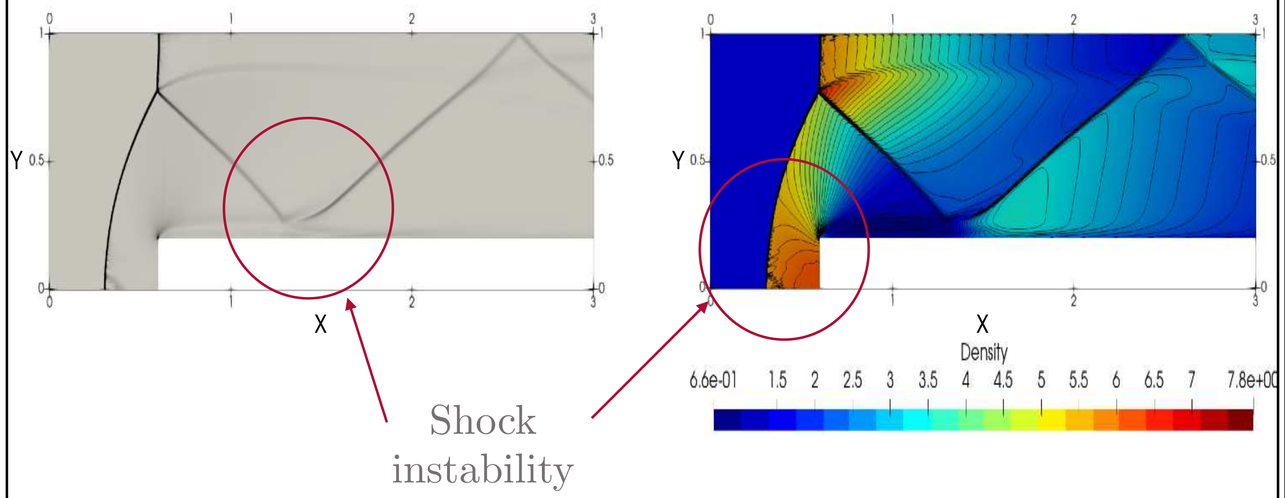

Multi-point solver Eul-0

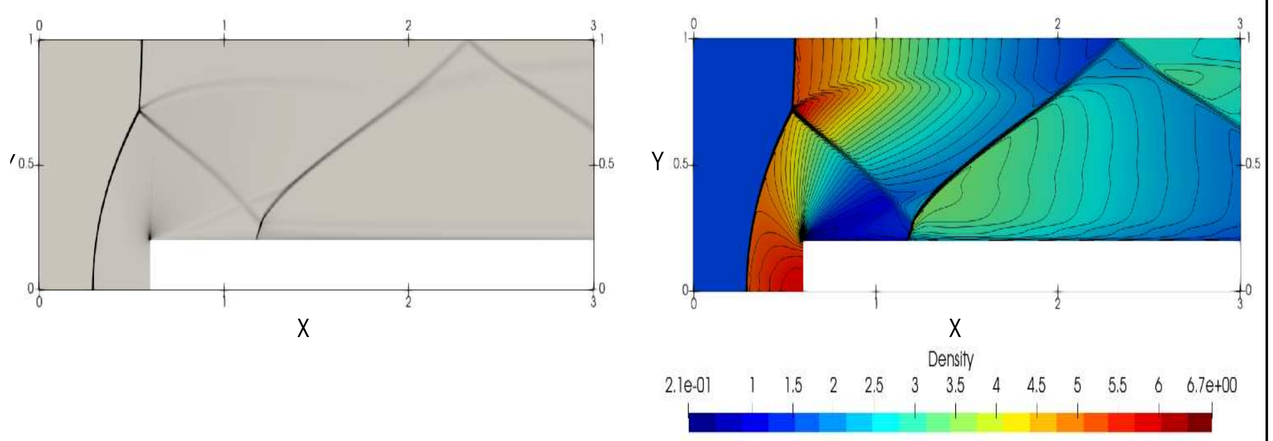

Two-point solver Eul-1

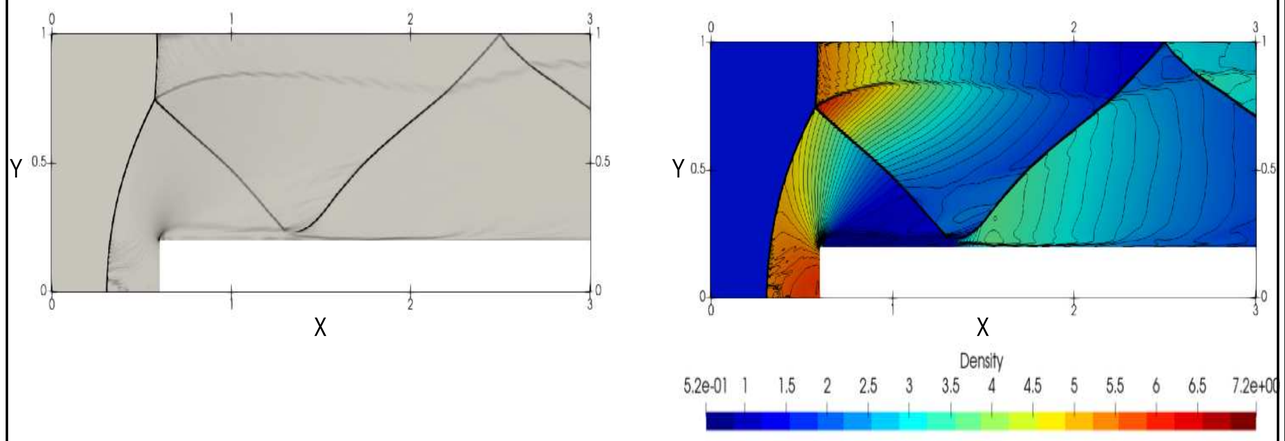

Multi-point solver Eul-1

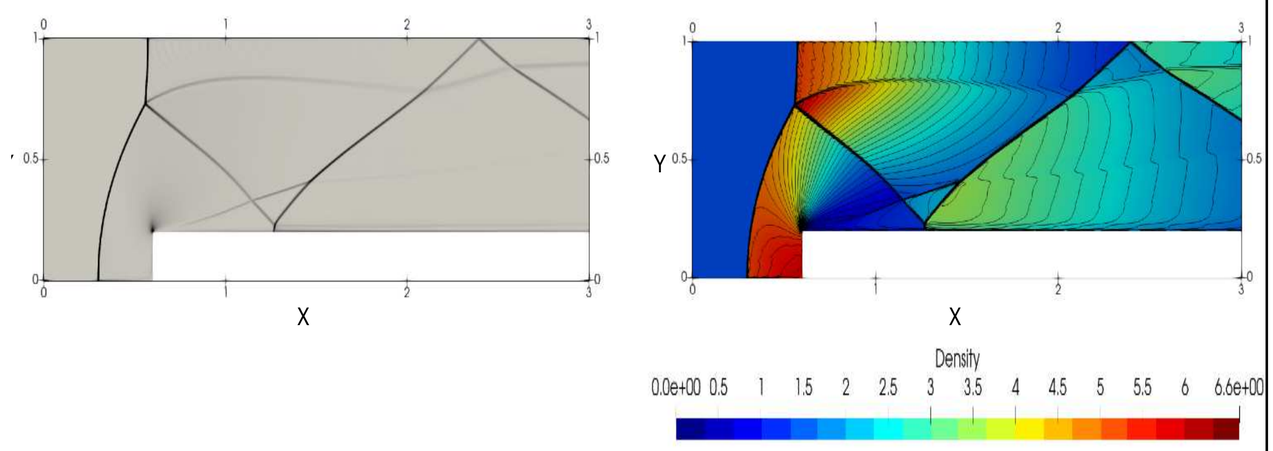

13. P. Woodward, P. Colella, The numerical simulation of two-dimensional fluid flow with strong shocks, Journal of Computational Physics(54), 1984.

Comparison of second-order two-point solver and multi-point solver.

Mach 2.032 planar shock wave and square cavity[14]

Two-point solver Eul-1

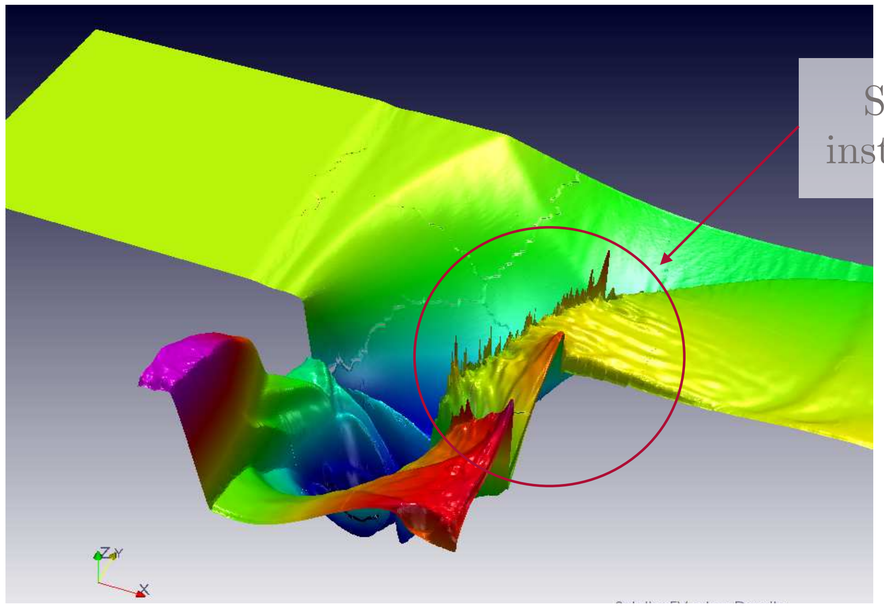

Multi-point solver Eul-1

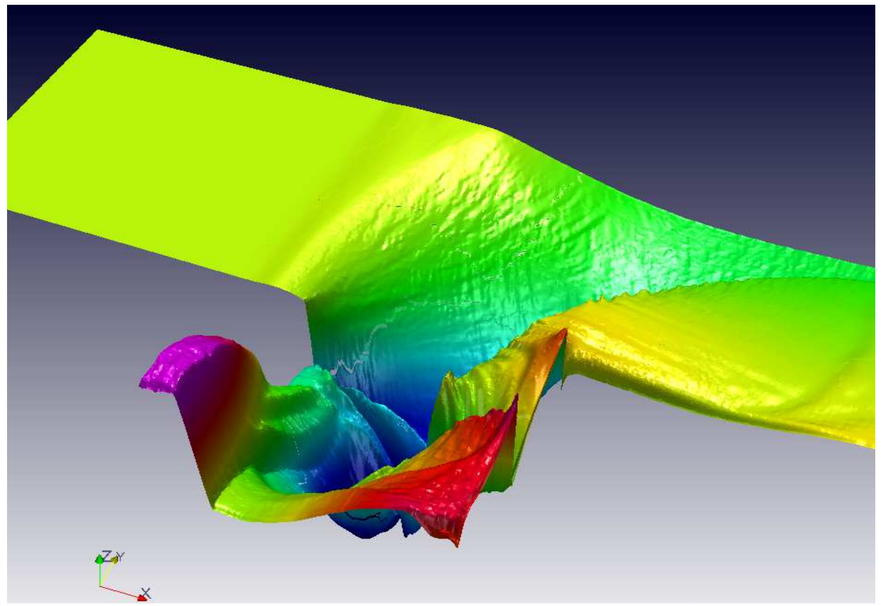

14. O. Ugra, J. Falcovitz, H. Reichenbach, W. Heilig, Experimental and numerical study of the interaction between a planar shock wave and a square cavity, J. Fluid Mech(313), 1996.

Extensions: 3D FV scheme and 2D axi-symmetric scheme

3D platform based on PETSc architecture

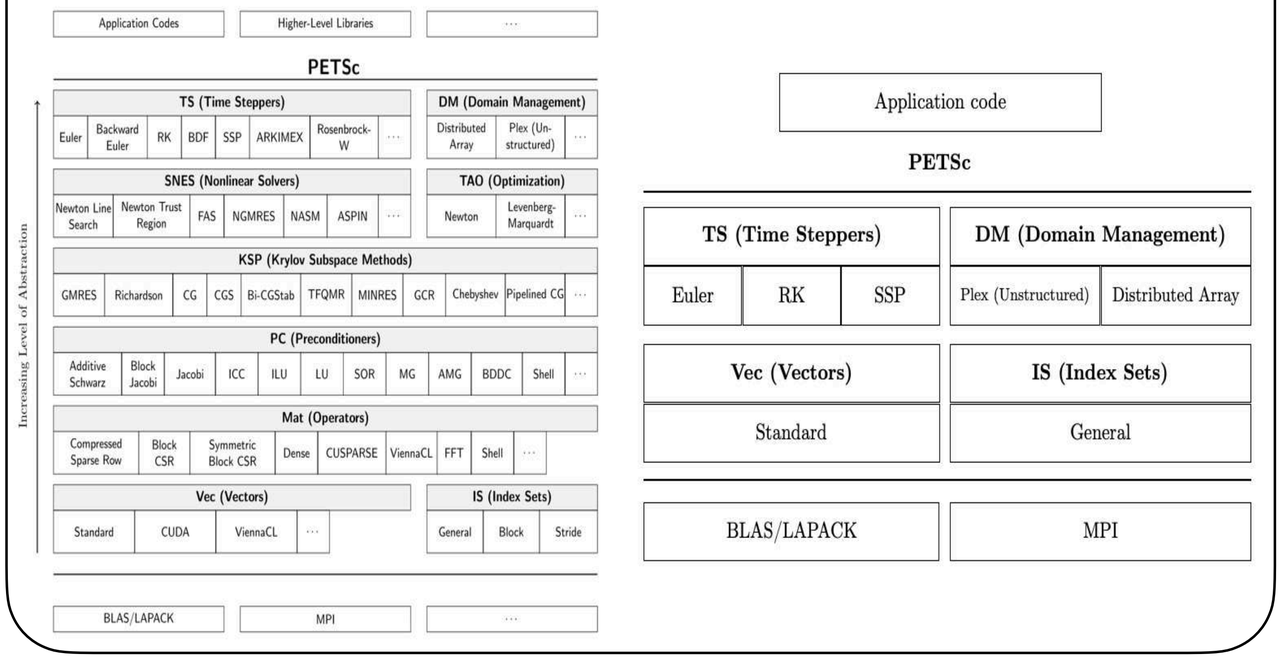

2D axysymmetric

$$(y\mathbf{u})_t + (y\mathbf{f})_x + (y\mathbf{g})_y = \mathbf{s}$$

$$\mathbf{u} = (\rho, \rho u, \rho v, \rho e)^t$$

$$\mathbf{f} = (\rho u, \rho u^2 + P, \rho uv, (\rho e + P)u)^t$$

$$\mathbf{g} = (\rho v, \rho uv, \rho v^2 + P, (\rho e + P)v)^t$$

$$\mathbf{s} = (0,0,P,0)^t$$

Add source term $(\mathbf{s} - \mathbf{g})/y$
in two-point and multi-point scheme.

Comparison of 3D and 2D axi-symmetric scheme.

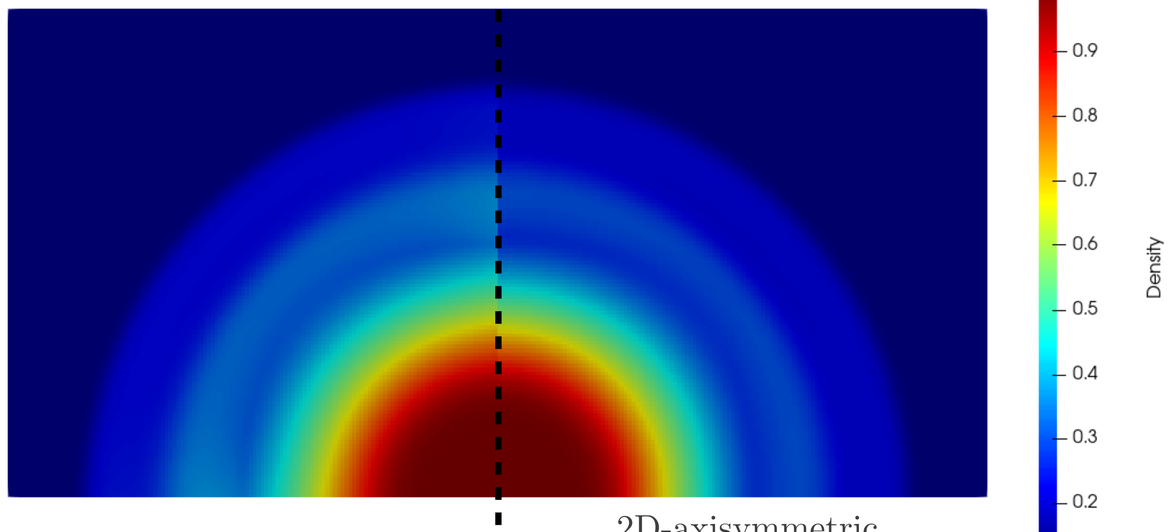

3D multi-point scheme
128^3 (N=2097152)
hexahedral cells

2D-axisymmetric
multi-point scheme
128^2 (N=16384)
quadrilateral cells

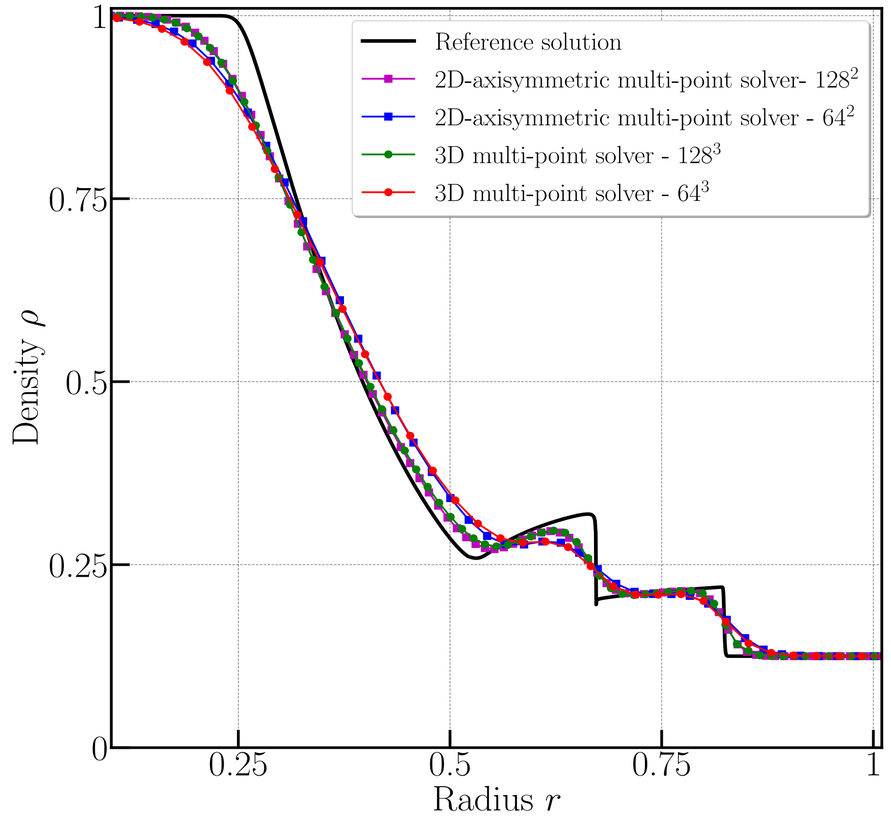

Sedov test case

Two-point solver

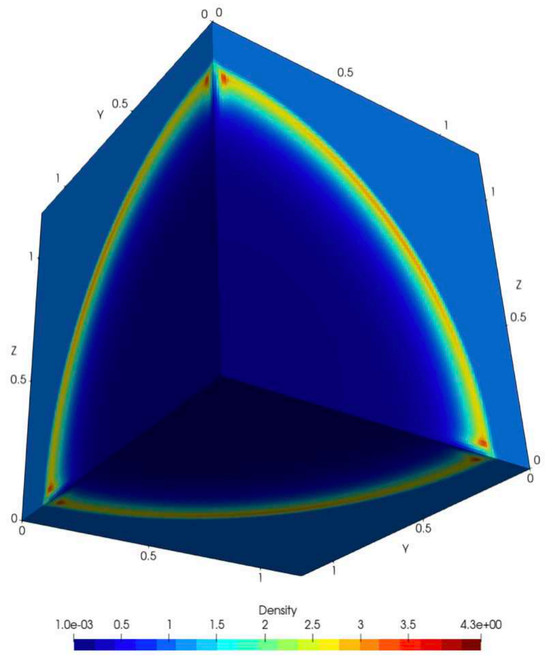

Multi-point solver

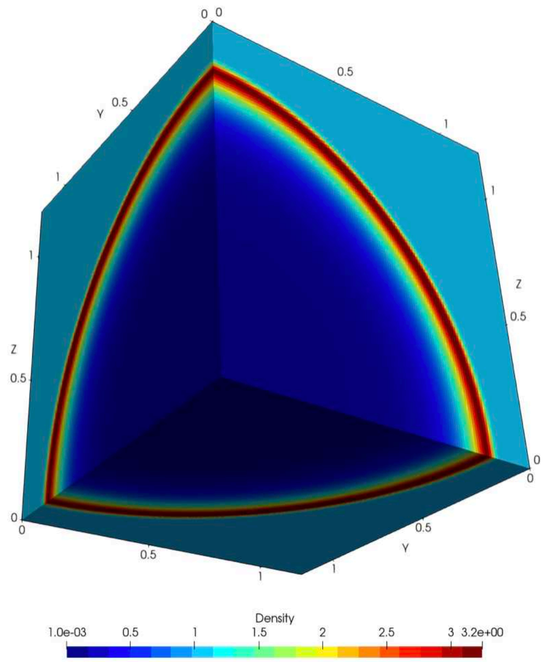

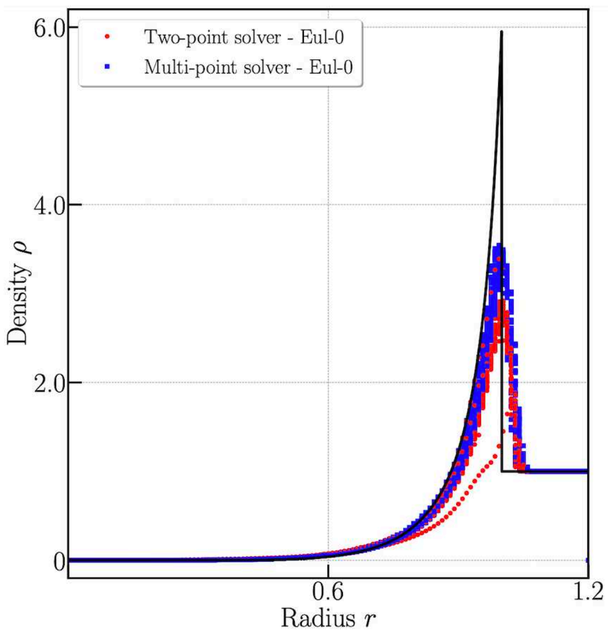

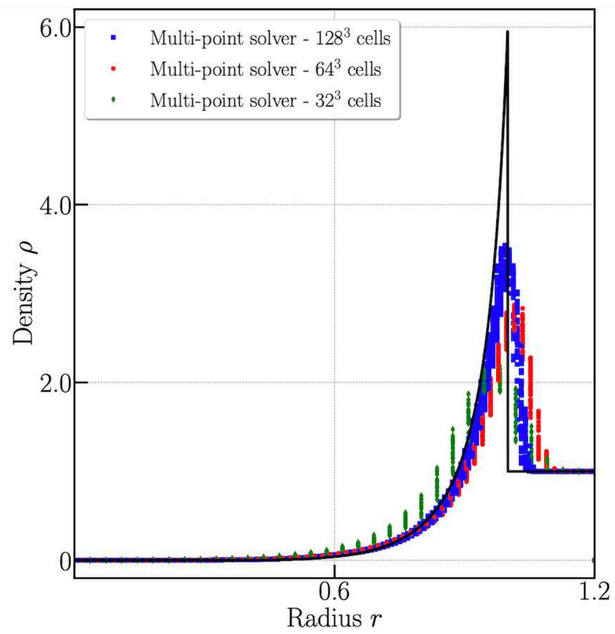

Comparison of 3D and 2D axi-symmetric scheme.

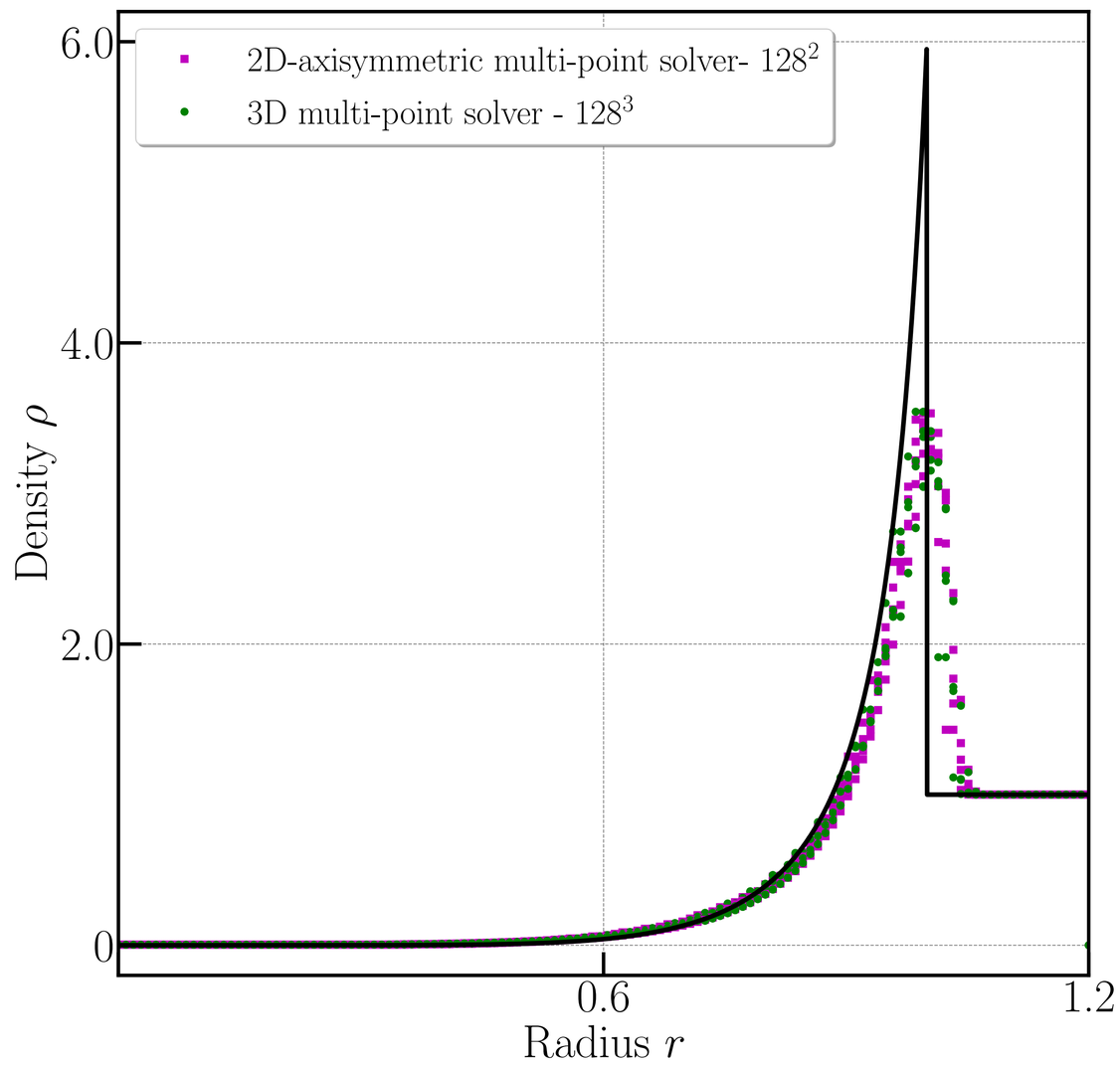

Mach 20 flow over sphere

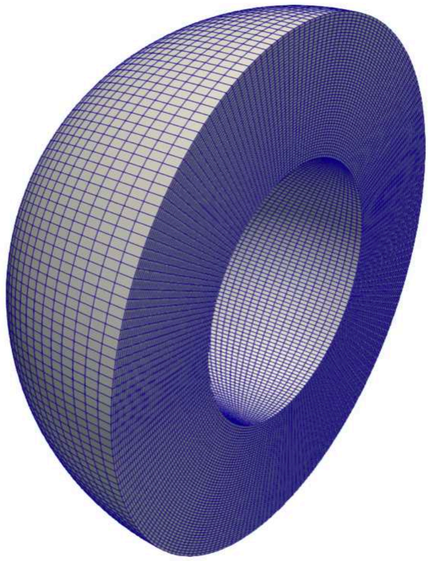

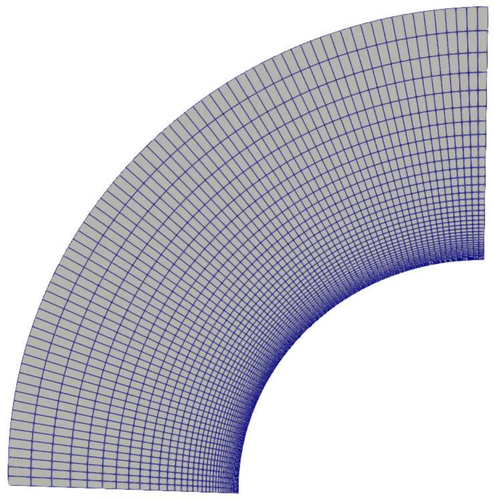

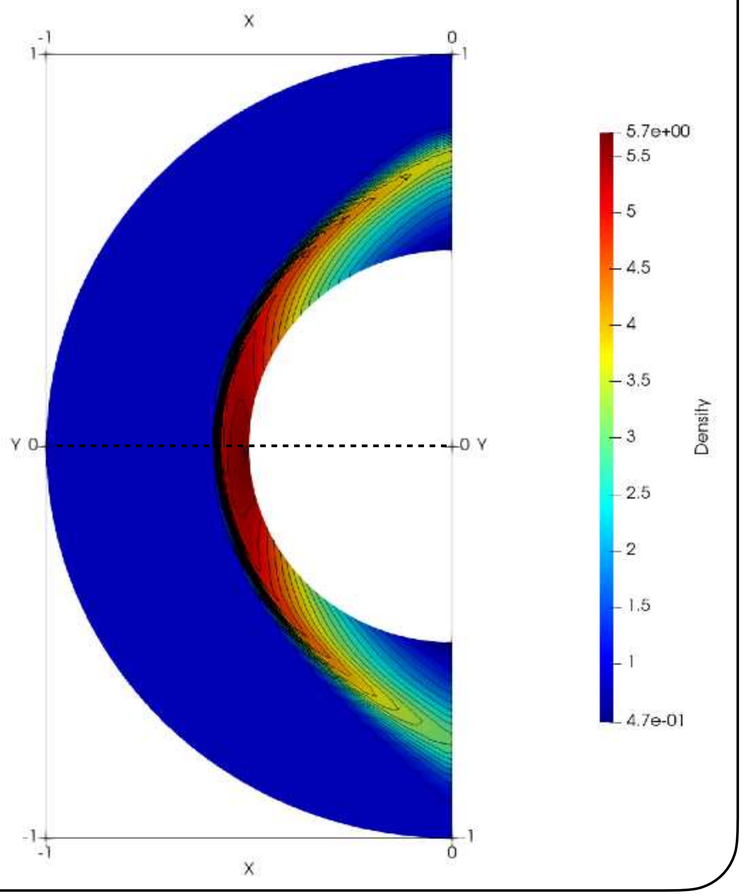

3D multi-point scheme

N = 255000
hexahedral cells

2D-axisymmetric multi-point scheme

N = 3000
quadrilateral cells

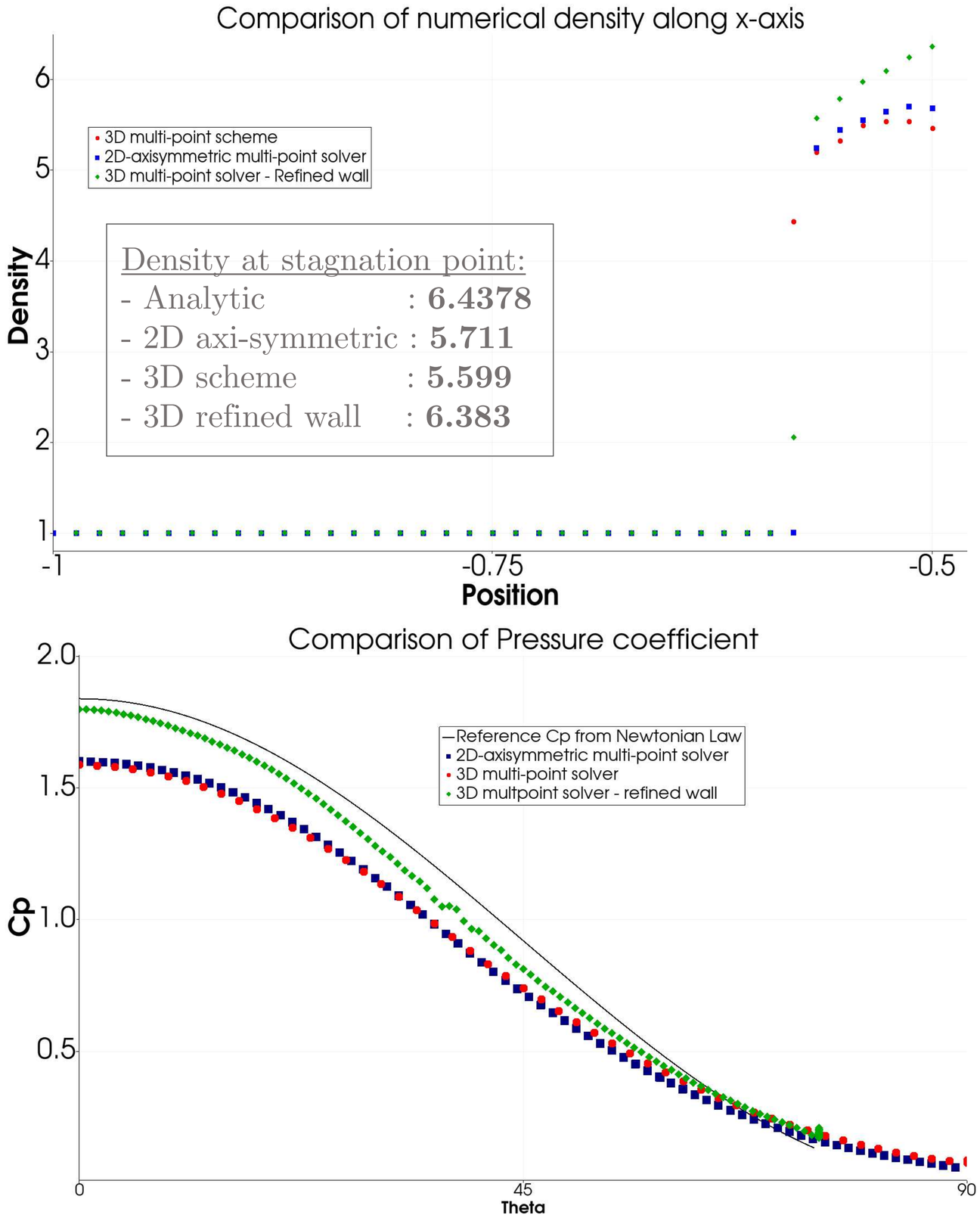

Blunted cone-flare test case[15]

Ma = 6; N = 1.5 million hexahedras (3D)

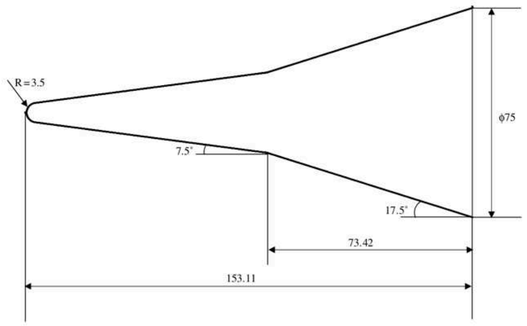

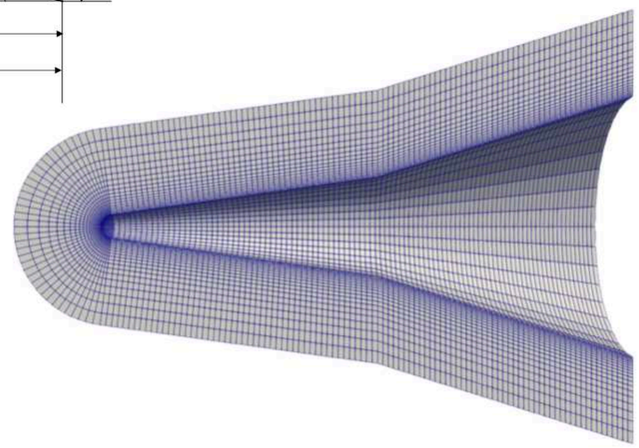

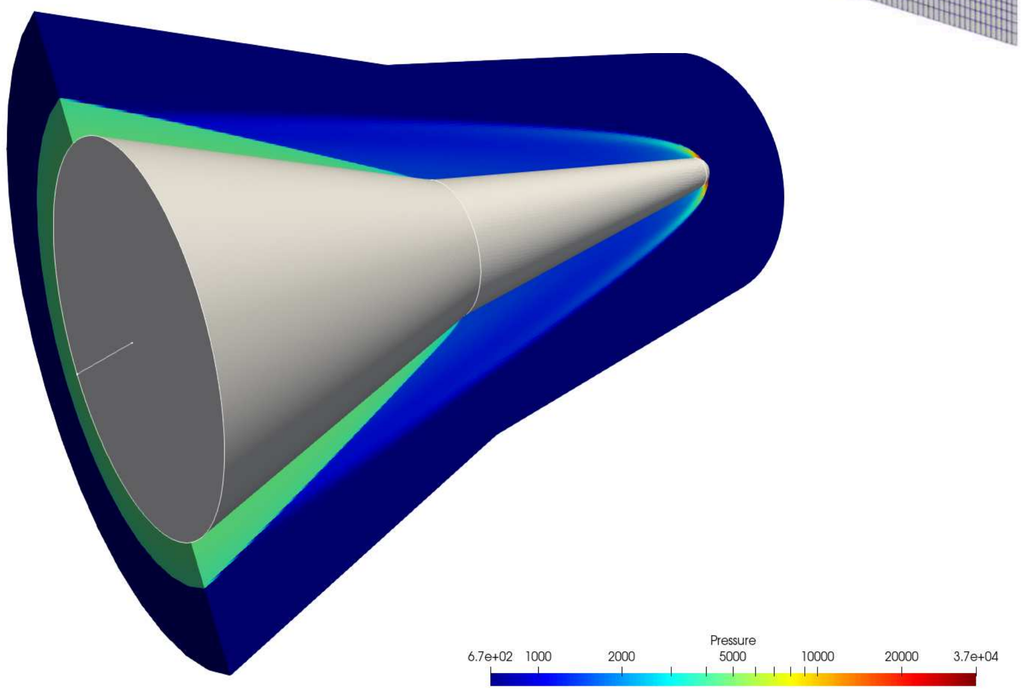

Comparison of our 3D solver and a structured 2D axisymmetric solver[16].

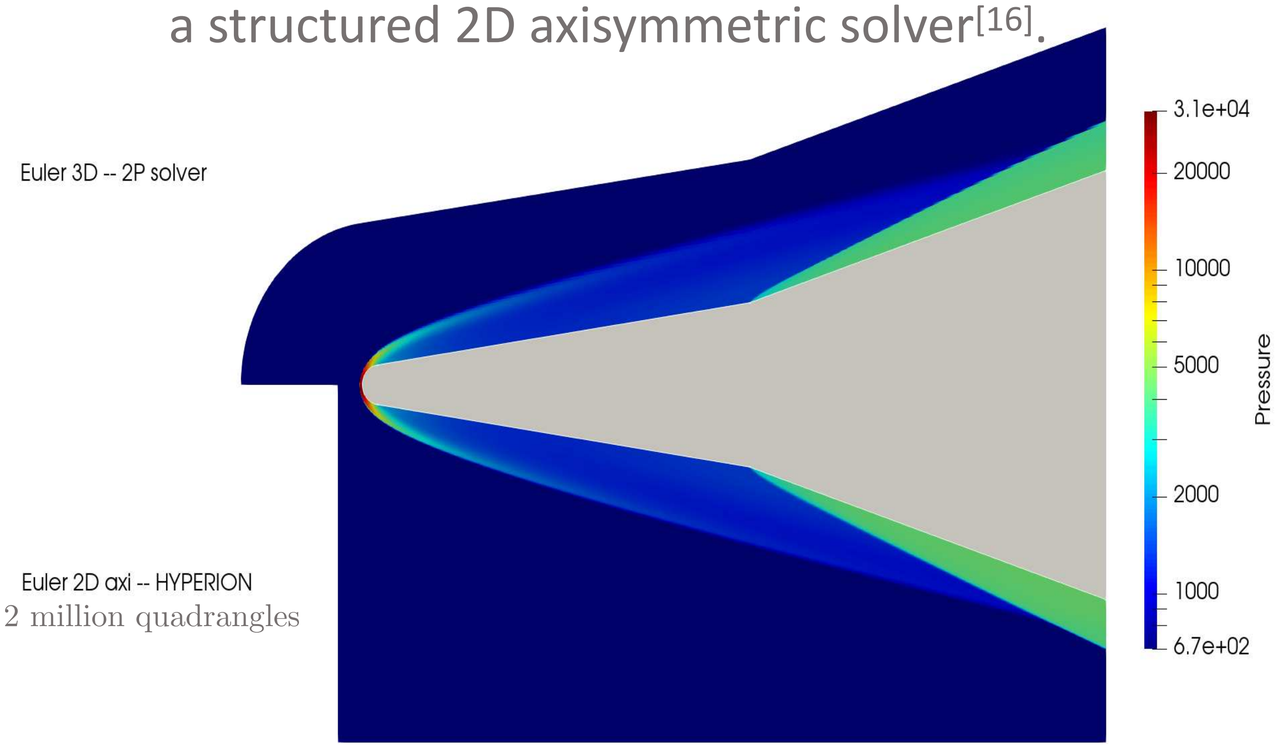

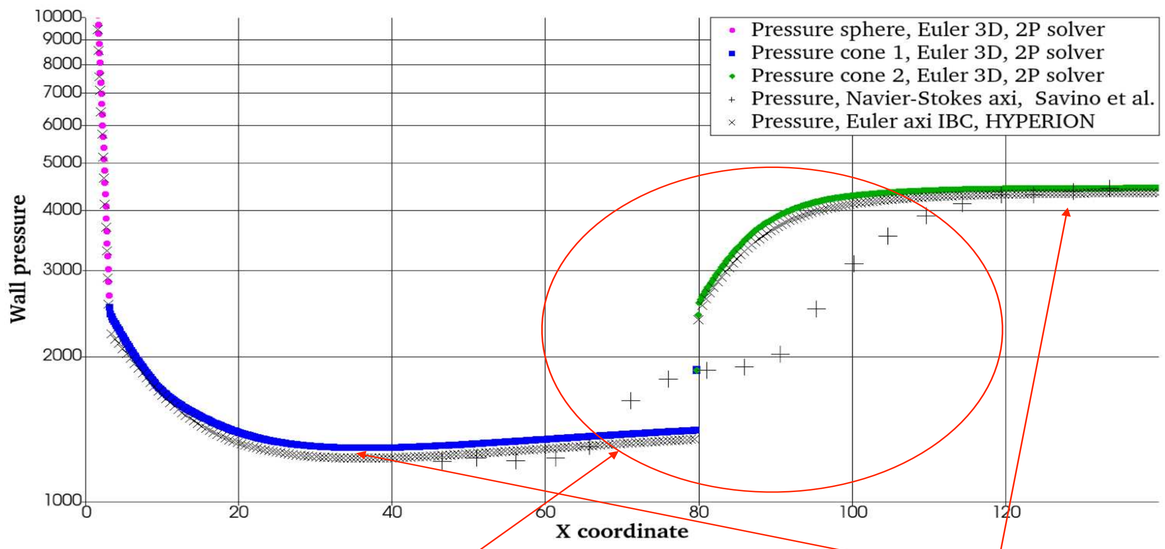

Recirculation zone

Eulerian code matches reference data when viscosity effect becomes small

15. R. Savinoo, D. Paterna, Blunted cone-flare in hypersonic flow, C&F 34, 2005.
16. T. Bridel-Bertomeu, Immersed boundary conditions for hypersonic flows using ENO-like least-square reconstruction, C&F 215, 2021

Maneuvrable Re-entry Vehicle (MaRV)[17]

Ma = 5; N = 11 million tetrahedra

Streamlines on bottom and top side are non-symmetrical.

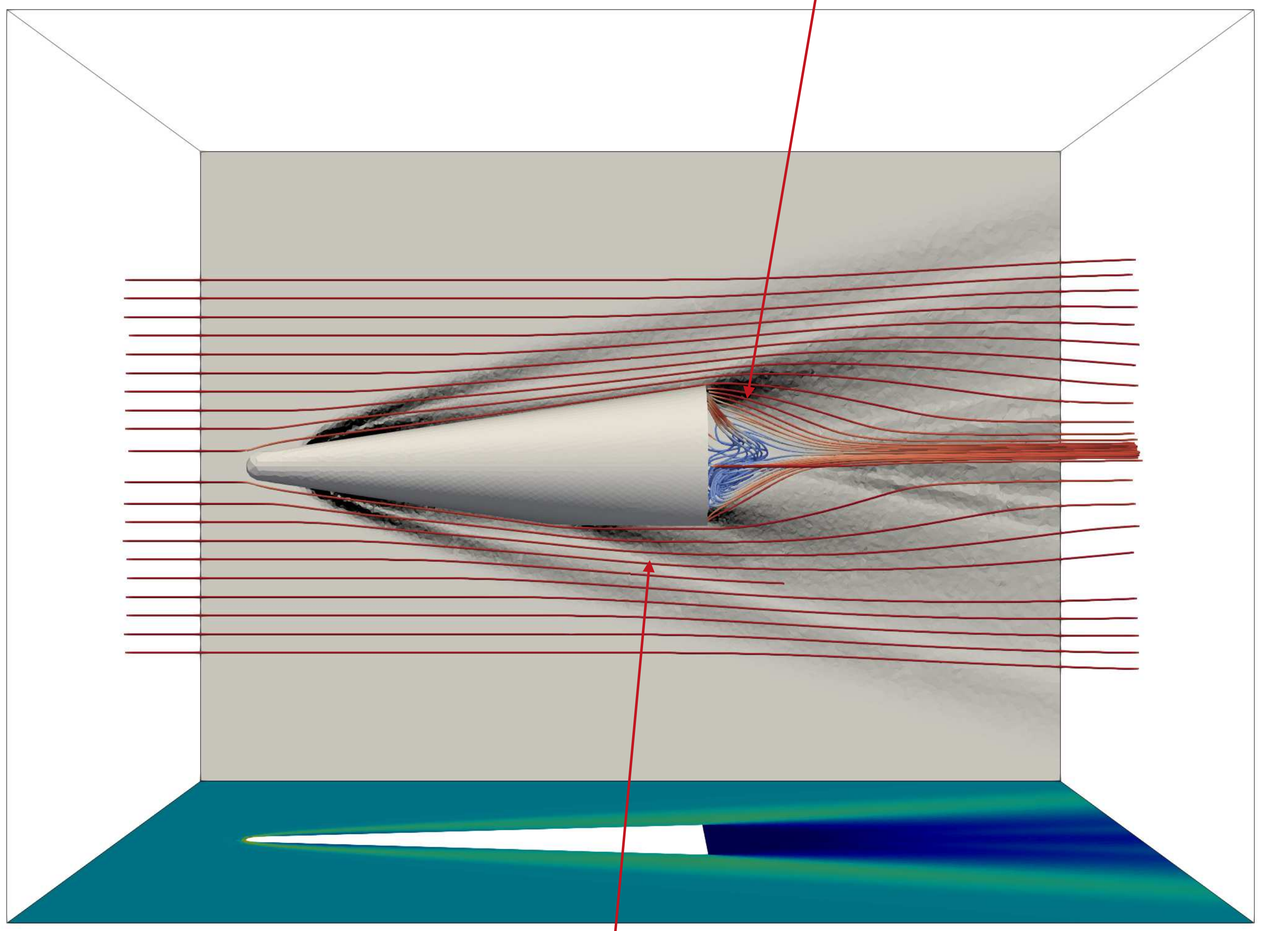

Extra rarefaction on bottom side.

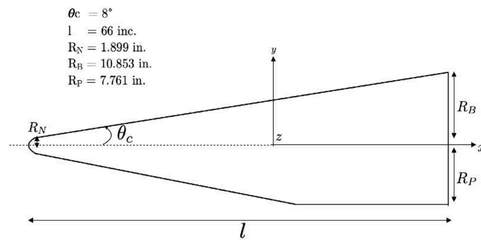

17.T. Petsopoulos, F. Regan, J. Barlow, Moving-mass roll control system for fixed-trim re-entry vehicle, Journal of Spacecraft and Rockets, 1996, 33(1),

Implicit scheme :

$$\frac{|\omega_c|}{\Delta t}\delta \mathbf{U}_c = -\mathbf{R}_c(\mathbf{U}^{n+1})$$

- Residual : $\mathbf{R}_c(\mathbf{U}) = \sum_{p\in\mathscr{P}(c)} \sum_{f\in\mathscr{SF}(pc} l_{pcf}\overline{\mathbf{F}}_{pcf},$

- $\delta \mathbf{U}_c = \mathbf{U}_c^{n+1} - \mathbf{U}_c^n.$

Define q as the Newton or nonlinear iteration counter :

$$\frac{|\omega_c|}{\Delta t}\underbrace{(\mathbf{U}_c^q + \delta\mathbf{U}_c^q}_{=\mathbf{U}_c^{q+1}} - \mathbf{U}_c^n) = \underbrace{-\mathbf{R}_c(\mathbf{U}^{q+1})}_{\text{Unknown}}.$$

Taylor expansion of $\mathbf{R}_c$:

$$\mathbf{R}_c(\mathbf{U}^{\mathbf{q+1}}) \approx \mathbf{R}_c(\mathbf{U}^q) + \left(\frac{\partial \mathbf{R}_c}{\partial \mathbf{U}_c}|_{\mathbf{U}_q}\right)\delta\mathbf{U}_c^q$$

Implicit scheme for steady state yields :

We want to find $\delta\mathbf{U} \to 0$, by setting $q = 0$:

$$\underbrace{\left[\frac{|\omega_c|}{\Delta t} + \frac{\partial \mathbf{R}_c(\mathbf{U}^n)}{\partial \mathbf{U}_c}\right]}_{\text{Implicit operator}}\delta\mathbf{U}_c = -\mathbf{R}_c(\mathbf{U}^n)\,.$$

Matrix form of the implicit operator :

$$\left(\frac{\mathbb{M}}{\Delta t} + \mathbb{E}\right)\delta\mathbf{U} = -\mathbf{R}_c(\mathbf{U}^n),$$

- Diagonal block-matrix : $\mathbb{M}$,
- Block matrix containing the Jacobian of numerical flux : $\mathbb{E}$.

Solving non-linear system :

- Iterative method : GMRES
- Preconditioning : ILU

Implicit numerical results : Mach 20 flow over half-cylinder

N = 5000 quads

Two-point scheme Multi-point scheme

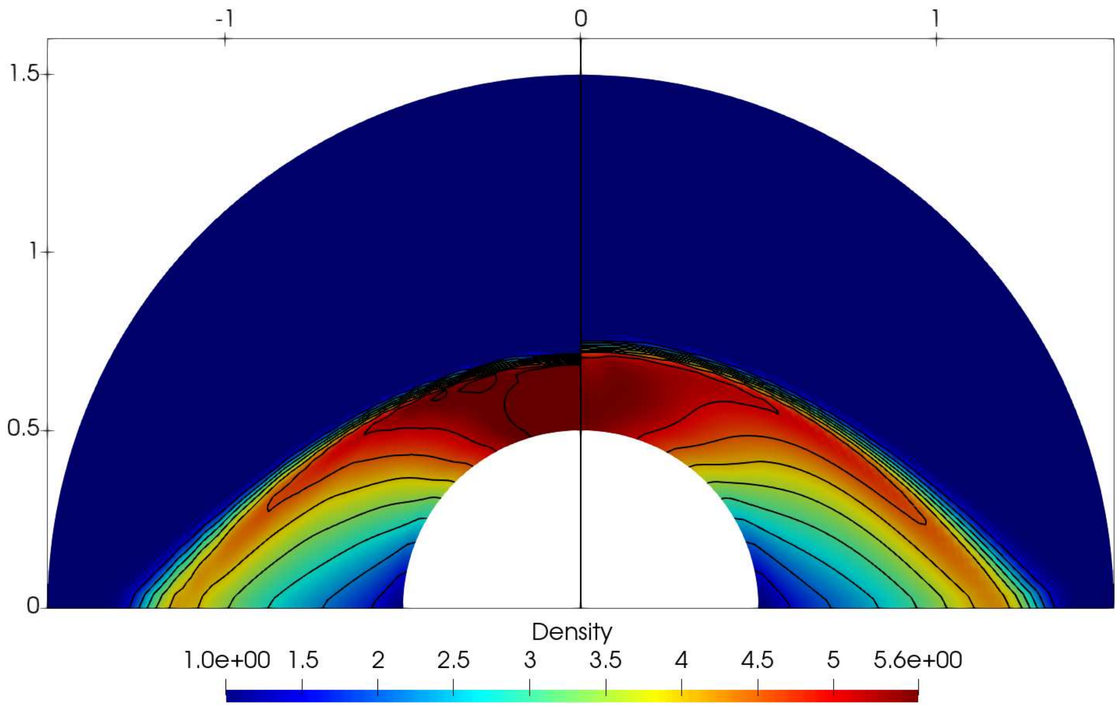

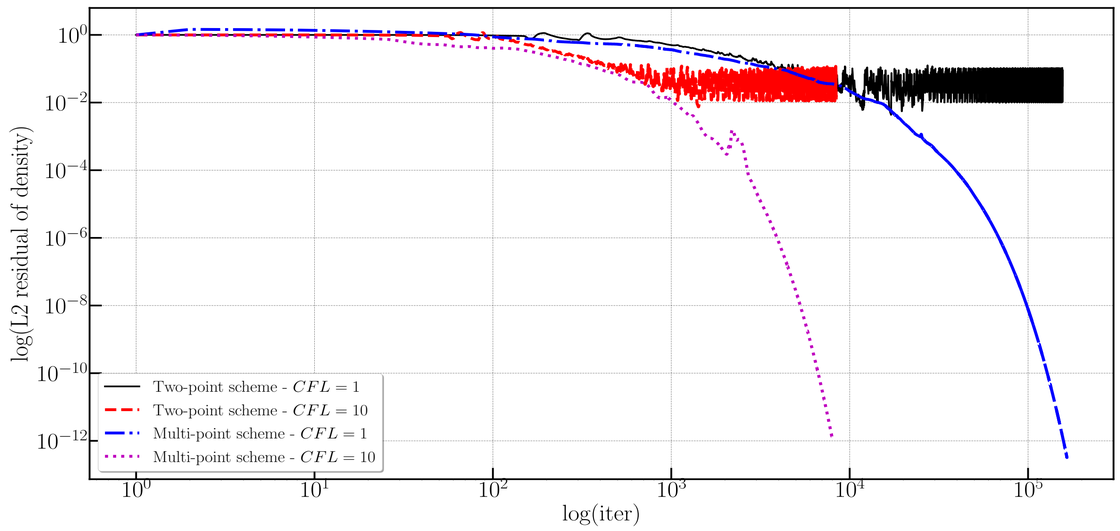

N = 5671 tris

Two-point scheme Multi-point scheme

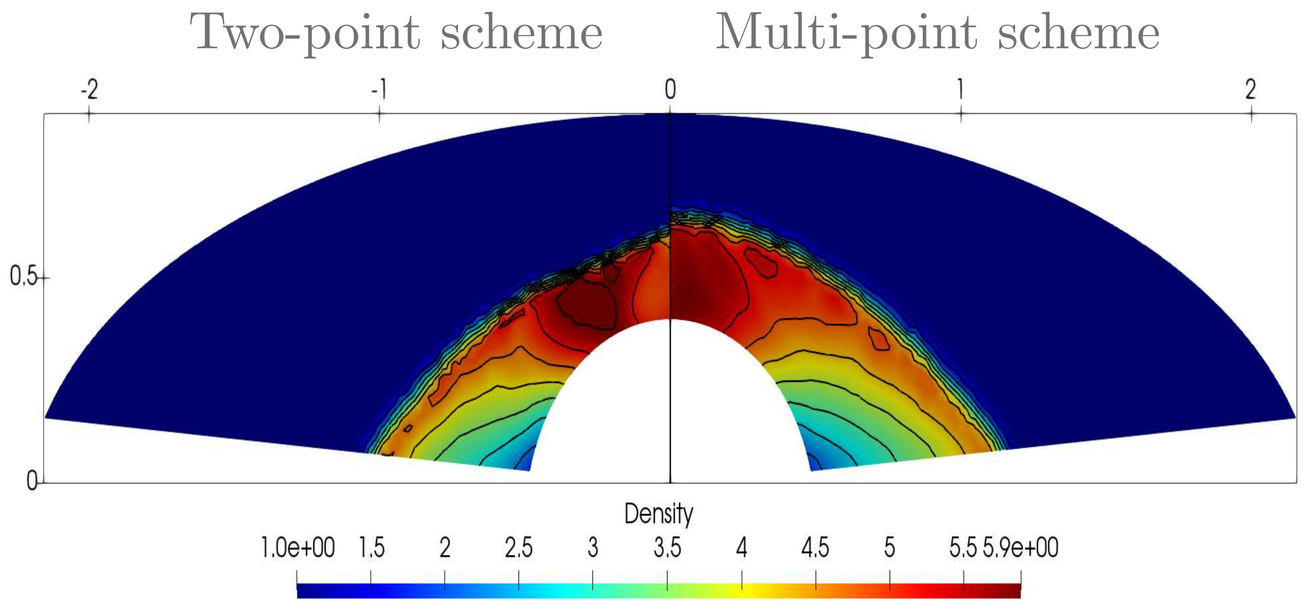

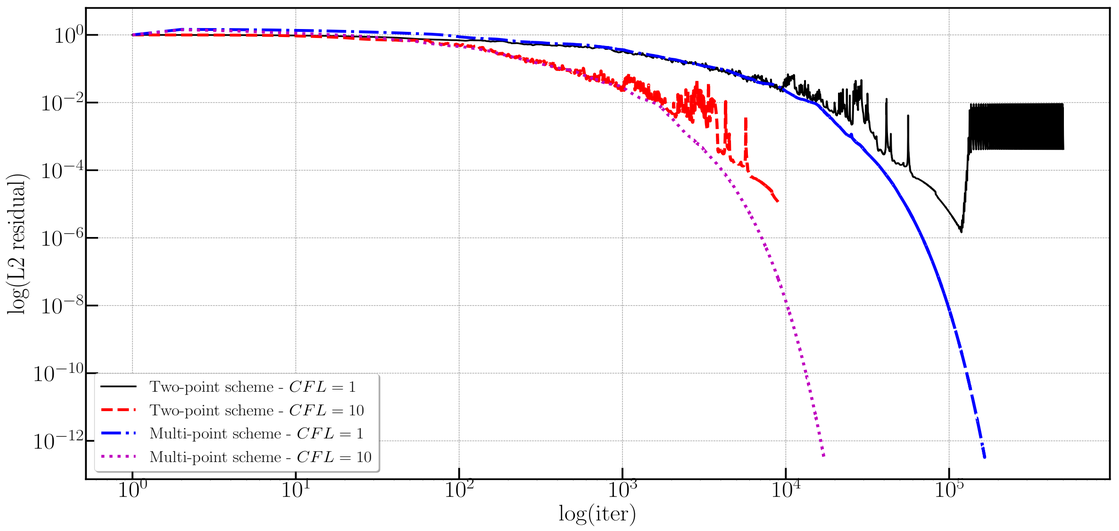

Implicit numerical results : Mach 6 flow over blunt cone-flare

N = 61494 tris

Pressure

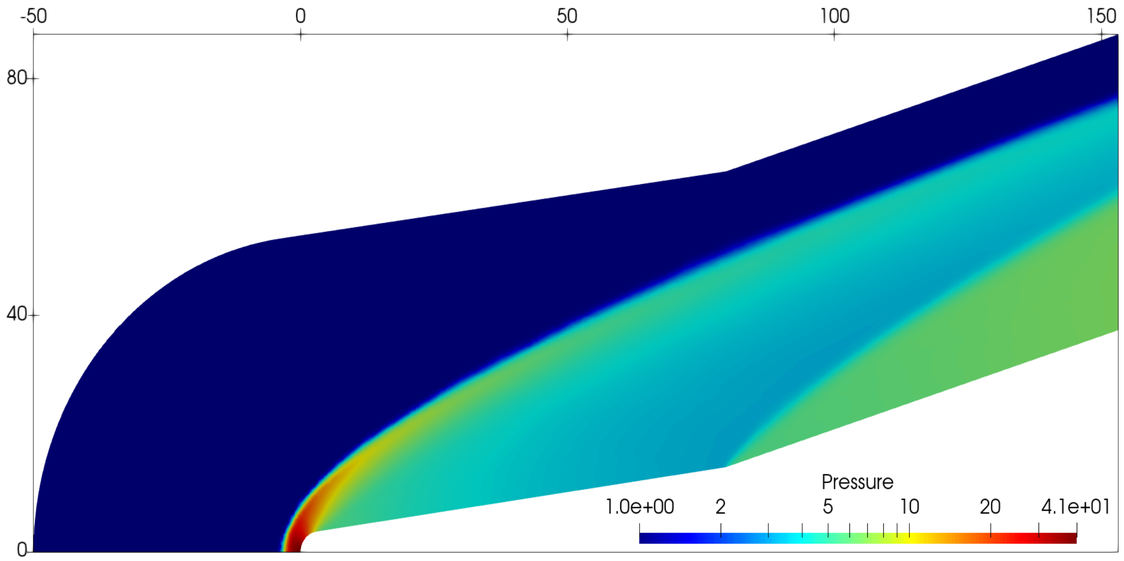

Density

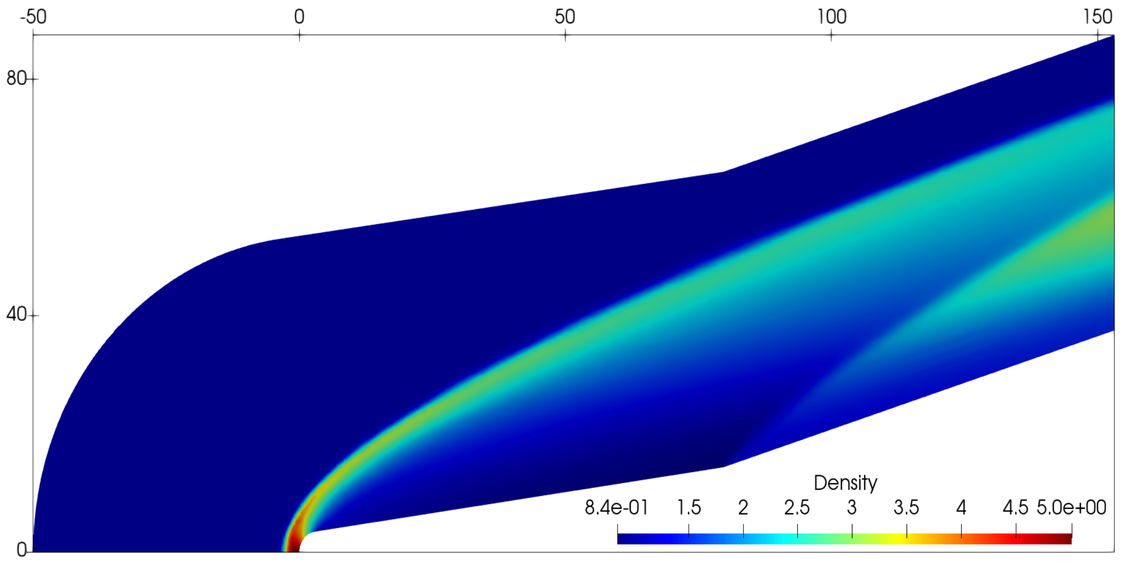

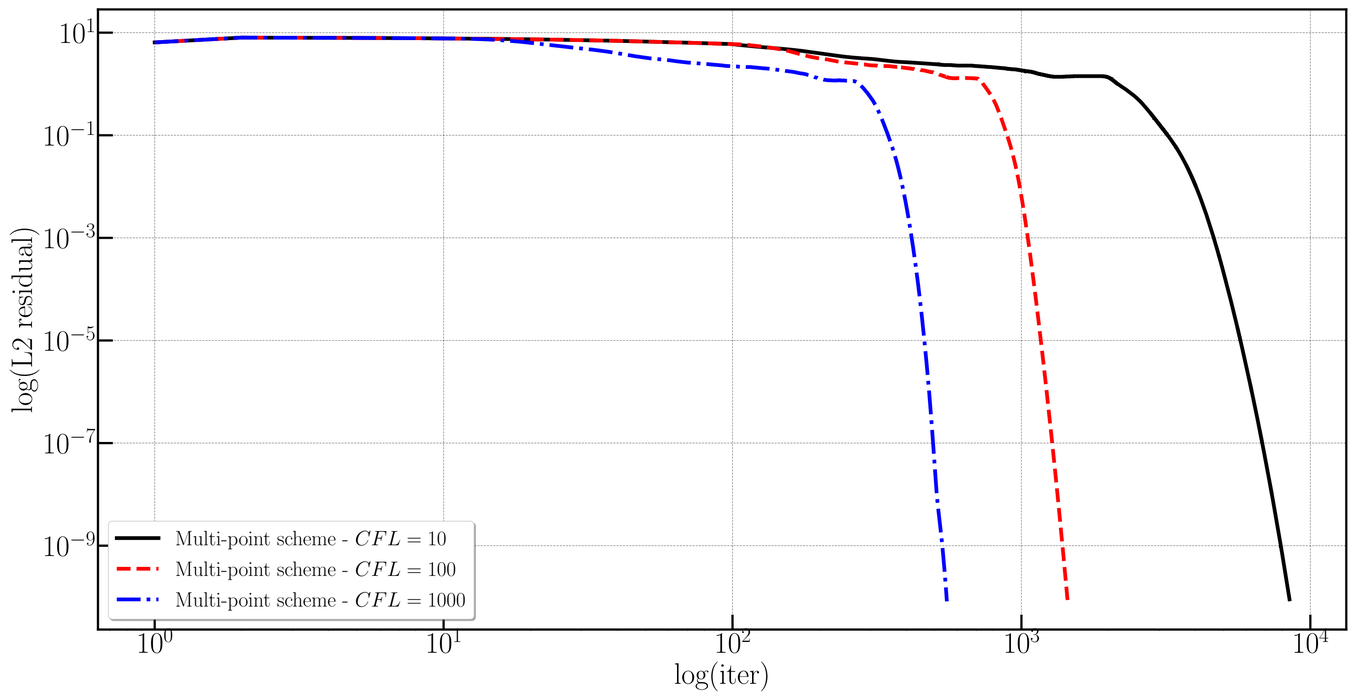

1D Lagrangian shallow water equations

$$\frac{\partial \mathbf{V}}{\partial t} + \frac{\partial}{\partial m}\mathbf{H}(\mathbf{V}) = \mathbf{P}(\mathbf{V}),$$

$$\mathbf{V} = (1/h, u)^t, \qquad \mathbf{H}(\mathbf{V}) = (-u, p)^t$$

$$\mathbf{P}(\mathbf{V}) = (0, -gh\partial_m B)^t$$

$$\text{Pressure} : p = g\frac{h^2}{2}$$

$$\text{Entropy inequality} : \frac{\partial}{\partial \tau}E + \frac{\partial}{\partial m}(pu) \leq -ghu\partial_m B$$

1D Eulerian shallow water equations

$$\frac{\partial \mathbf{U}}{\partial t} + \frac{\partial}{\partial x}\mathbf{F}(\mathbf{U}) = \mathbf{S}(\mathbf{U}),$$

$$\mathbf{U} = (h, hu)^t, \quad \mathbf{F}(\mathbf{U}) = (hu, hu^2 + p)^t$$

$$\mathbf{S}(\mathbf{U}) = (0, -gh\partial_x B)^t$$

Construction of simple well-balanced Lagrangian solver:

$$\mathbf{W}(\frac{m}{t}, \mathbf{V}_l, \mathbf{V}_r) = \begin{cases} \mathbf{V}_l & \text{if} \quad \frac{m}{t} \leq -\lambda_l, \\ \mathbf{V}_l^\star & \text{if} \quad -\lambda_l \leq \frac{m}{t} < 0, \\ \mathbf{V}_r^\star & \text{if} \quad 0 < \frac{m}{t} \leq \lambda_r, \\ \mathbf{V}_r & \text{if} \quad \frac{m}{t} \geq \lambda_r. \end{cases}$$

With $\mathbf{V}_s^\star = (\frac{1}{h_s^\star}, u_s^\star)$

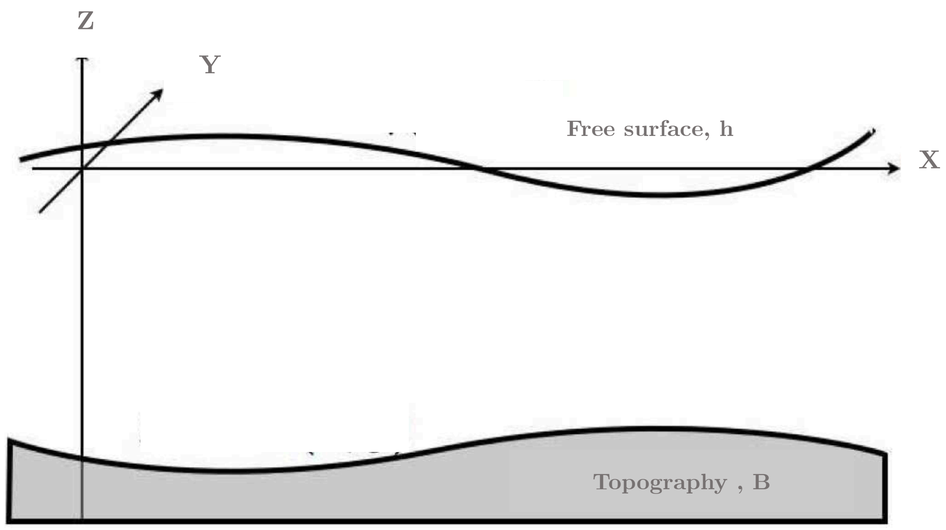

Consistency of the Riemann solver :

$$-\lambda_l(\mathbf{V}_l^\star - \mathbf{V}_l) + \lambda_r(\mathbf{V}_r - \mathbf{V}_r^\star) = \Delta\mathbf{H} - \Delta m\mathbf{P},$$

Where $\overline{h\Delta B} = \Delta m\overline{h\partial_m B}$

Jump relations :

$$u_l^\star - \lambda_l\frac{1}{h_l^\star} = u_l - \lambda_l\frac{1}{h_l},$$

$$u_l^\star = u_r^\star,$$

$$u_r^\star + \lambda_r\frac{1}{h_r^\star} = u_r - \lambda_r\frac{1}{h_r},$$

Compute intermediate states $u_s^\star$, $h_s^\star$

Lake at rest stationary solution,
$u_l = u_r = 0, h_l + B_l = h_r + B_r = \eta$ constant :

$$g\overline{h\Delta B} = -(p_r - p_l).$$

We set $\overline{h\Delta B} = h(B_r - B_l)$, provided that
$\overline{h} = \frac{1}{2}(h_r + h_l)$

Lagrangian numerical flux :

$$\mathbf{H}^\star = \frac{1}{2}(\mathbf{H}_l + \mathbf{H}_r) - \frac{\lambda_l}{2}(\mathbf{V}_l^\star - \mathbf{V}_l) - \frac{\lambda_r}{2}(\mathbf{V}_r - \mathbf{V}_r^\star).$$

Lagrange-to-Euler mapping:

$$\Lambda_l = u_l - \lambda_l\frac{1}{h_l}, \Lambda_O = u^\star, \Lambda_r = u_r + \lambda_r\frac{1}{h_r}$$

Eulerian numerical flux :

$$\mathbf{F}^\star = \frac{1}{2}(\mathbf{F}_l + \mathbf{F}_r) - \frac{\Lambda_l}{2}(\mathbf{U}_l^\star - \mathbf{U}_l) - \frac{\Lambda_0}{2}(\mathbf{U}_r^\star - \mathbf{U}_l^\star) - \frac{\Lambda_r}{2}(\mathbf{U}_r - \mathbf{U}_r^\star).$$

Extensions: Shallow water equations 1D Numerical results

Subcritical flow

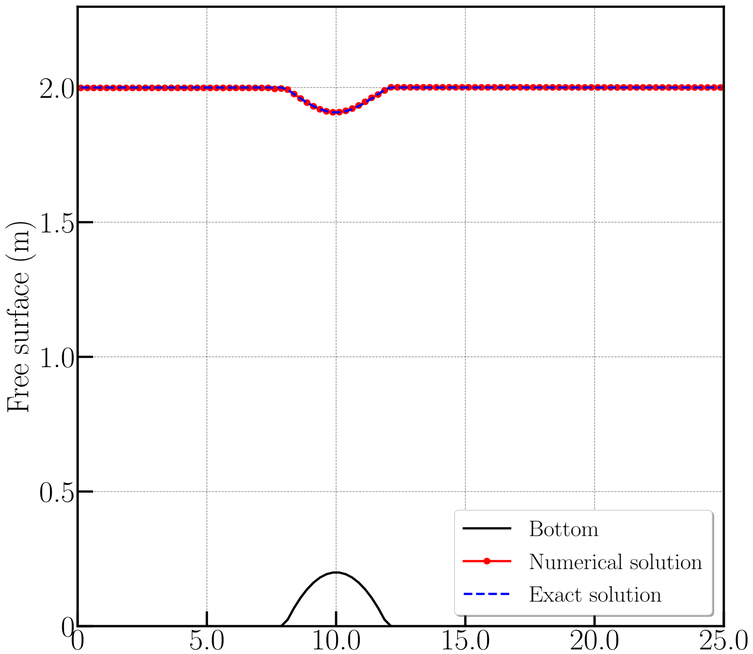

Supercritical flow

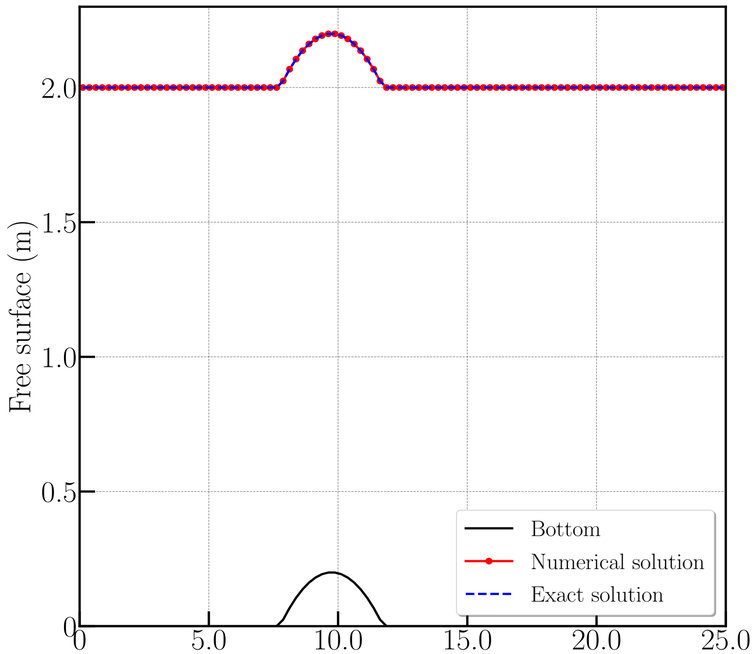

Transcritical flow

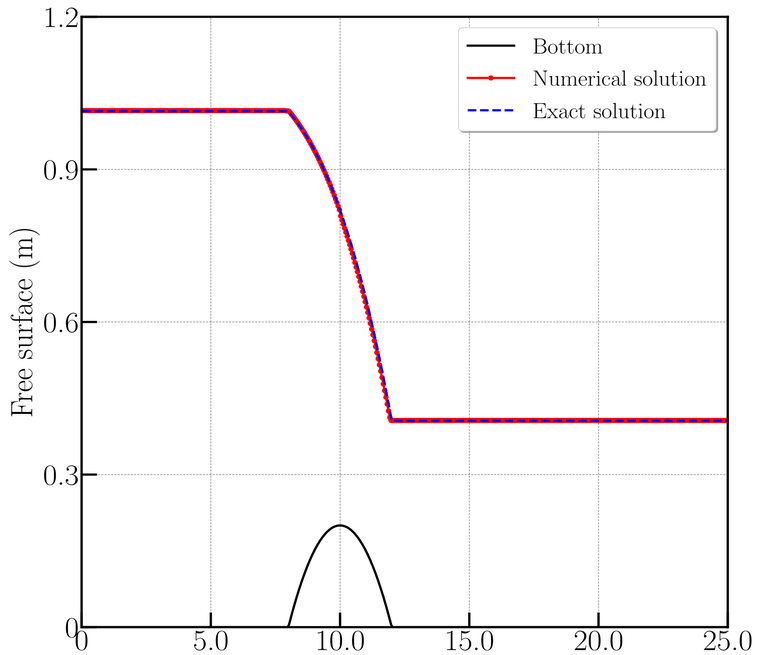

Modified dry bed - Positivity-preserving validation

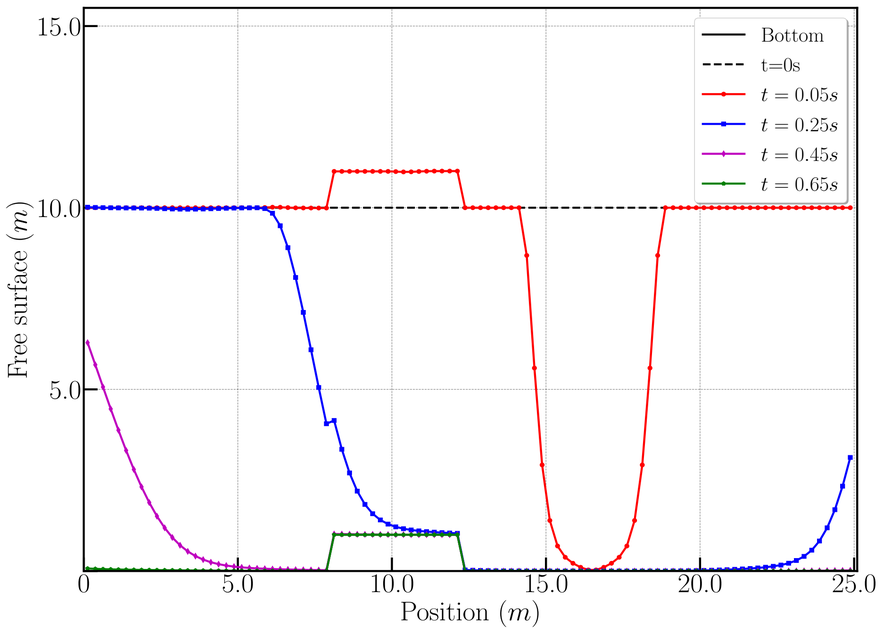

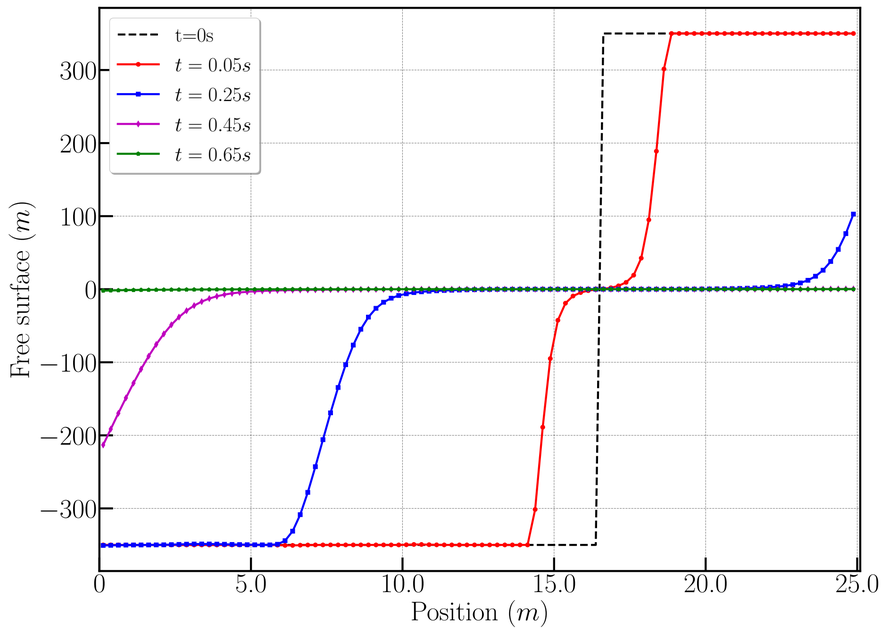

Lake at rest over 3 mounds :

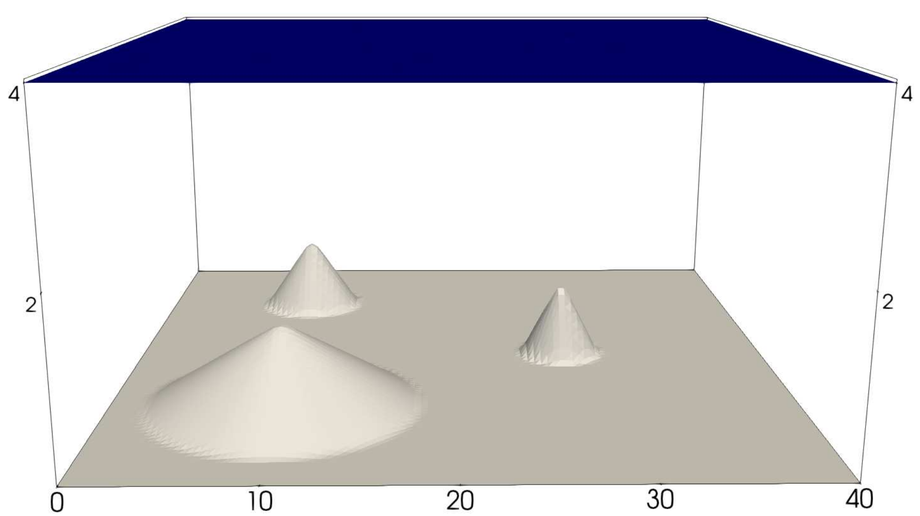

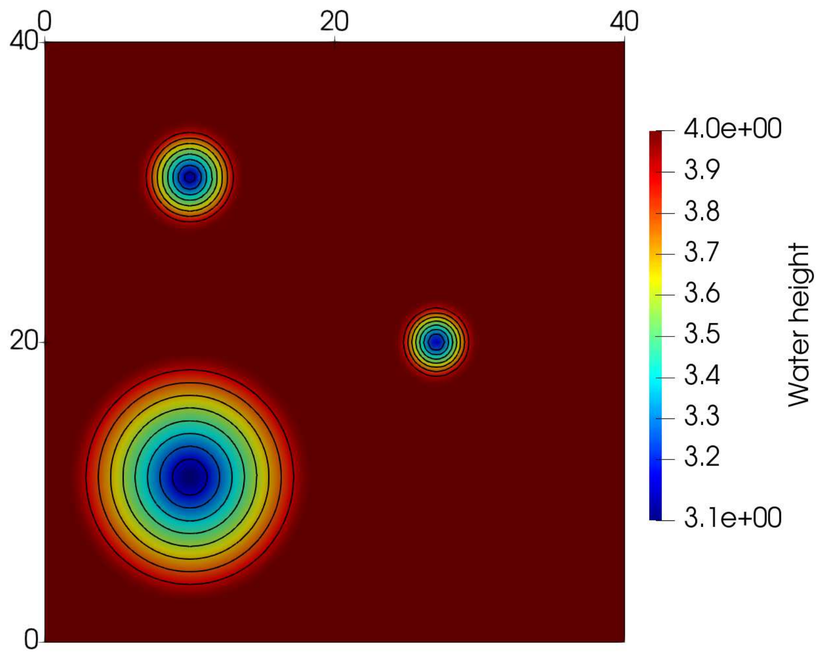

Quirk test case :

Two-point solver

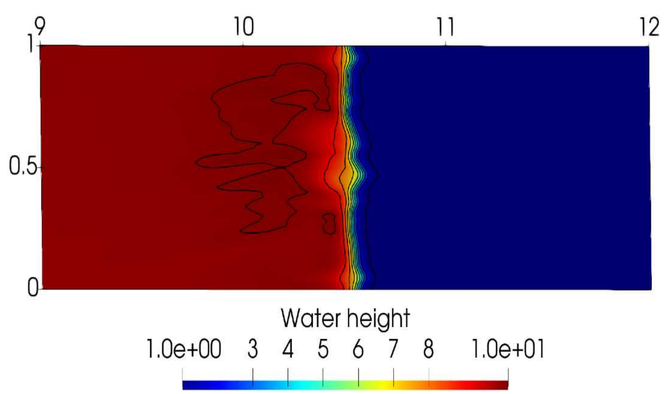

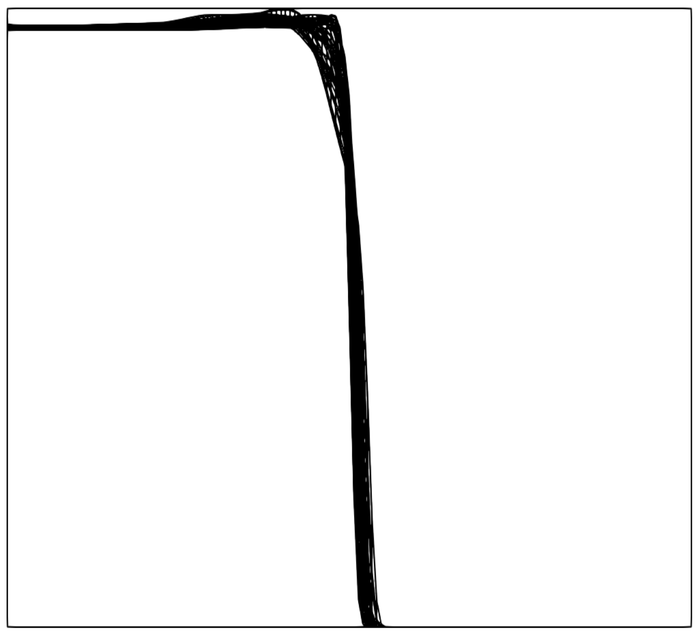

Multi- point solver

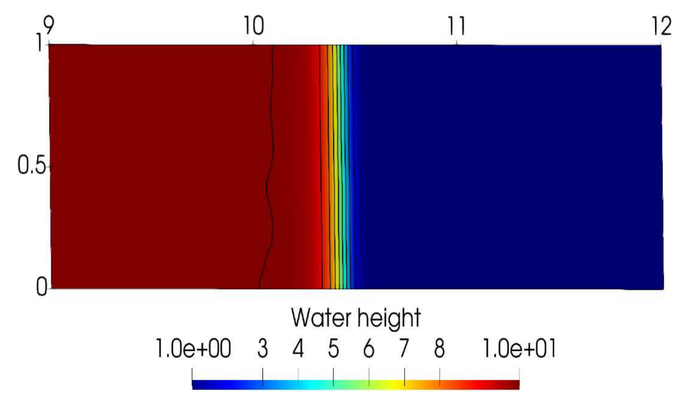

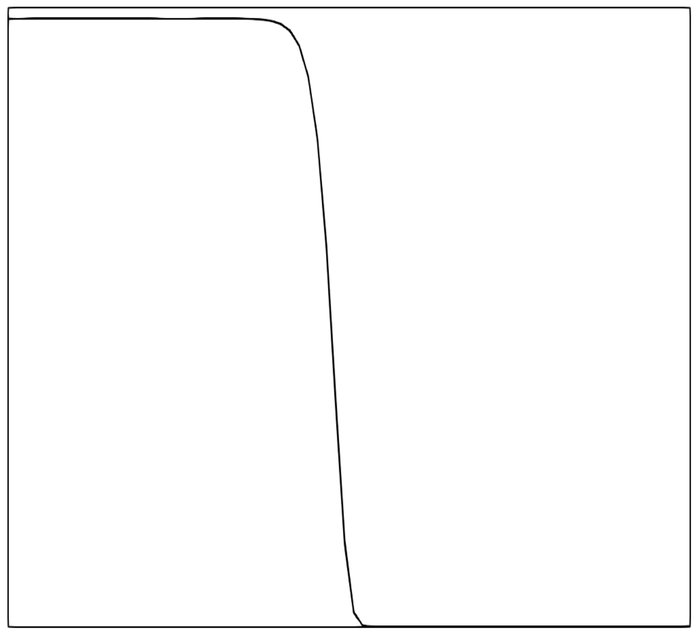

Conclusion

1. Novel class of subface-based FV scheme for hyperbolic systems.
2. Subface numerical flux with non conservative approximate Riemann solvers.
3. Simple Lagrangian Riemann solver and Eulerian counterpart thanks to Lagrange-to-Euler mapping.
4. Node-based conservation and entropy condition.
5. Positivity and entropy stability under explicit time step condition;.
6. FV scheme less sensitive to instabilities.
7. Gas dynamics application.
8. Extensions : 3D, implicit time discretization, shallow water equations.

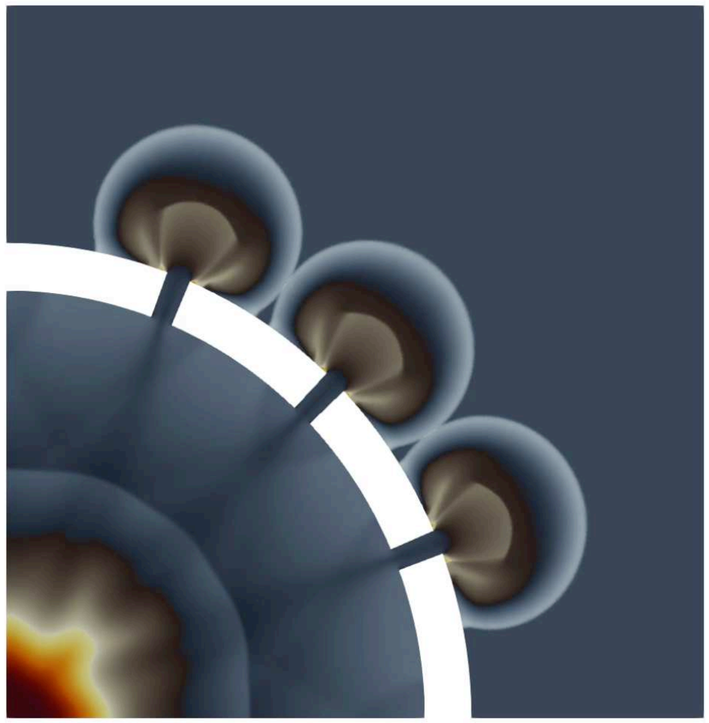

Perspective :

1. Extension to complex physics : MHD, multi-material flows etc.
2. Navier-Stokes equations.
3. Real gas.

Comparison of two-point solver and multi-point solver.

Cylindrical Sod shock tube

Comparison of numerical density and internal energy

(40000 quadrilateral cells)

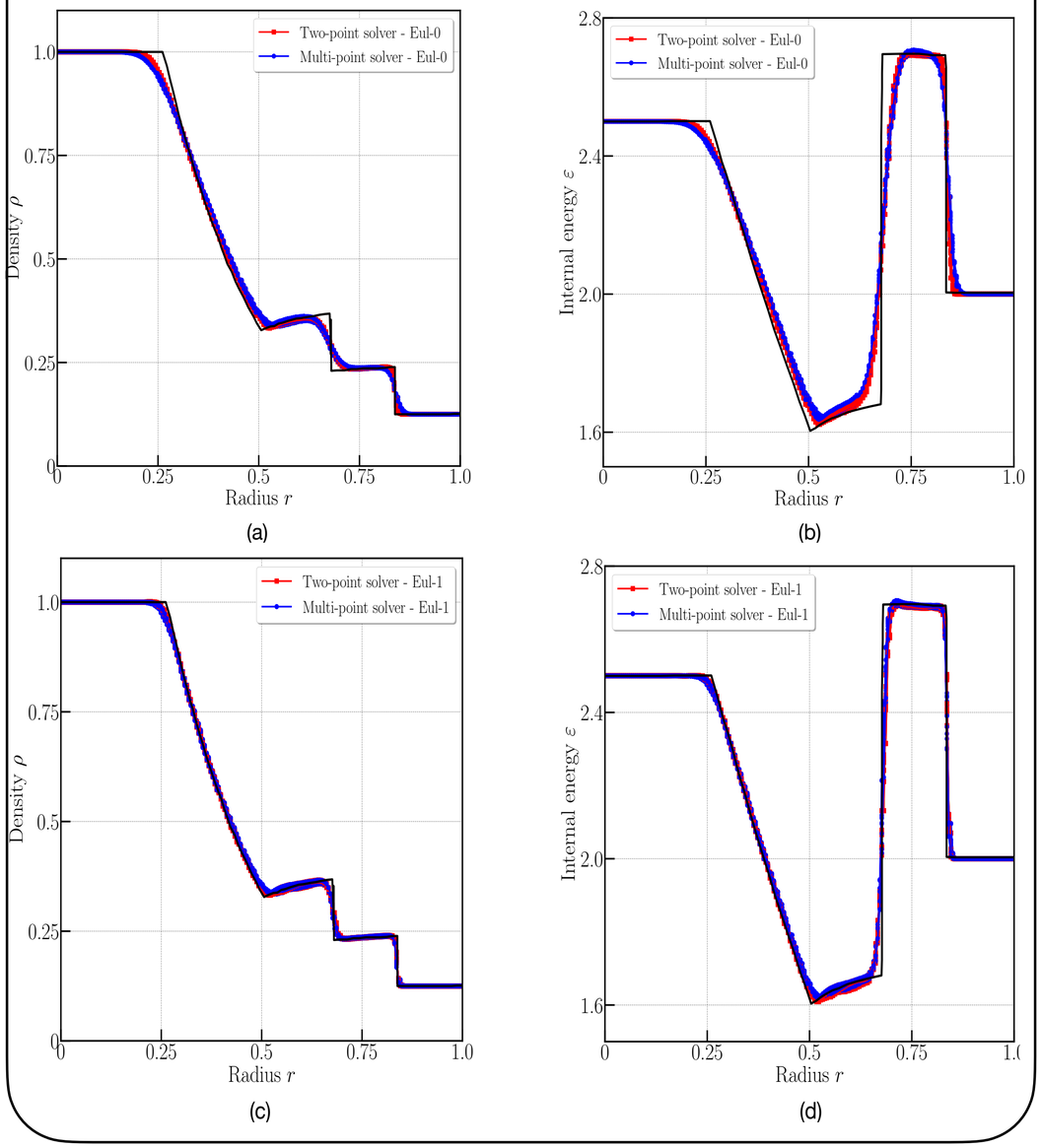

CPU time decomposition

Two-point scheme										
Order	CPU time [s]	N. Iter	Init.	Time per iteration[s] (CPU deocmposition [%])						Efficiency [µs/iter/cell]
				Time step	P1 recon.	Limiter	Residual		u_i^{n+1}	
							States	RS		
1 (Eul-0)	38.7	847	2.32s (6%)	0.397s (1%)	-	-	0.032s (69%)	0.01s (22%)	0.0009s (2%)	1.104
2 (Eul-1)	148.65s	895	1.48s (1%)	0.002s (1%)	0.091s (55%)	0.018s (11%)	0.042s (25%)	0.009s (6%)	0.002s (1%)	4.011

Multi-point scheme										
Order	CPU time [s]	N. Iter	Time per iteration[s] (CPU deocmposition [%])							Efficiency [µs/iter/cell]
			Time step	Nodal solver			P1 recon.	Limiter	Residual		u_i^{n+1}	
				States	Dukowicz	Nodal velocity			States	RS		
1	176.51s	829	1.765s (1%)	0.066s (26%)	0.023s (11%)	0.066s (31%)	-	-	0.043s (20%)	0.021s (10%)	0.002s (1%)	5.14
2	391.28s	845	3.913s (1%)	0.107s (23%)	0.027s (6%)	0.148s (32%)	0.088s (19%)	0.019s (4%)	0.046s (10%)	0.019s (4%)	0.005s (1%)	11.184